

General aspects of effective field theories and few-body applications

Hans-Werner Hammer and Sebastian König

Abstract Effective field theory provides a powerful framework to exploit a separation of scales in physical systems. In these lectures, we discuss some general aspects of effective field theories and their application to few-body physics. In particular, we consider an effective field theory for non-relativistic particles with resonant short-range interactions where certain parts of the interaction need to be treated nonperturbatively. As an application, we discuss the so-called *pionless effective field theory* for low-energy nuclear physics. The extension to include long-range interactions mediated by photon and pion-exchange is also addressed.

1 Introduction: dimensional analysis and the separation of scales

Effective field theory (EFT) provides a general approach to calculate low-energy observables by exploiting scale separation. The origin of the EFT approach can be traced to the development of the renormalization group [1] and the intuitive understanding of ultraviolet divergences in quantum field theory [2]. A concise formulation of the underlying principle was given by Weinberg [3]: If one starts from the most general Lagrangian consistent with the symmetries of the underlying theory, one will get the most general S-matrix consistent with these symmetries. As a rule, such a most general Lagrangian will contain infinitely many terms. Only together with a power counting scheme that orders these terms according to their importance at low energies one obtains a predictive paradigm for a low-energy theory.

The Lagrangian and physical observables are typically expanded in powers of a low-momentum scale M_{lo} , which can be a typical external momentum or an internal infrared scale, over a high-momentum scale $M_{\text{hi}} \gg M_{\text{lo}}$.¹ This expansion provides the basis for the power counting scheme. It depends on the system to which physical scales M_{hi} and M_{lo} correspond to.

As an example, we take a theory that is made of two particle species, two light bosons with mass M_{lo} and heavy bosons with mass $M_{\text{hi}} \gg M_{\text{lo}}$.² We consider now soft processes in which the energies and momenta are of the order of the light particle mass (the so-called soft scale).

Hans-Werner Hammer

Institut für Kernphysik, Technische Universität Darmstadt, 64289 Darmstadt, Germany, e-mail: Hans-Werner.Hammer@physik.tu-darmstadt.de,

Sebastian König

Department of Physics, The Ohio State University, Columbus, Ohio 43210, USA e-mail: koenig.389@osu.edu

¹ Note there are often more than two scales, which complicates the power counting. Here we focus on the simplest case to introduce the general principle.

² For further examples, see the lectures by Kaplan [4, 5].

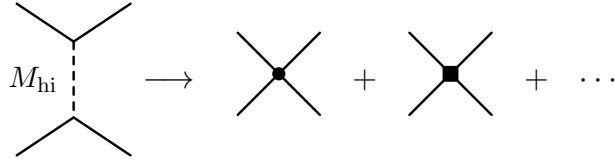


Fig. 1 Expansion of heavy-particle exchange between light particles in terms of contact interactions between light particles. The solid and dashed lines denote light and heavy particles, respectively. The circle and square denote contact interactions with zero and two derivatives, in order.

Under such conditions, the short-distance physics related to the heavy particles can never be resolved explicitly. However, it can be represented by light-particle contact interactions with increasing dimension (number of derivatives). To illustrate this, we consider the scattering of the light particles mediated by heavy-particle exchange, with g the heavy-light coupling constant. The corresponding interaction Lagrangian is given by

$$\mathcal{L}_{\text{int}} = g (\chi^\dagger \phi \phi + \phi^\dagger \phi^\dagger \chi), \quad (1)$$

where ϕ denotes the light boson field and χ is the heavy boson field. As depicted in Fig. 1, one can represent such exchange diagrams by a sum of local operators of the light fields with increasing number of derivatives. In a symbolic notation, the leading order scattering amplitude can be written as

$$T \sim \frac{g^2}{M_{\text{hi}}^2 - q^2} = \frac{g^2}{M_{\text{hi}}^2} + \frac{g^2 q^2}{M_{\text{hi}}^4} + \dots, \quad (2)$$

with q^2 the squared 4-momentum transfer. We will come back to this example in more detail in section 2.

In many cases, the corresponding high-energy theory is either not known or can not easily be solved. Still, EFT offers a predictive and systematic framework for performing calculations in the light-particle sector. We denote by Q a typical energy or momentum of the order of M_{lo} and by M_{hi} the hard scale where the EFT will break down. In many cases, this scale is set by the masses of the heavy particles not considered explicitly and thus replaced by contact interactions as in the example above. In such a setting, any matrix element or Green's function admits an expansion in the small parameter Q/M_{hi} [3]

$$\mathcal{M} = \sum_{\mathbf{v}} \left(\frac{Q}{M_{\text{hi}}} \right)^{\mathbf{v}} \mathcal{F} \left(\frac{Q}{\Lambda}, g_i \right) \quad (3)$$

where \mathcal{F} is a function of order one (this is the naturalness assumption), Λ a regularization scale (related to the UV divergences appearing in the loop graphs) and the g_i denotes a collection of coupling constants, often called low-energy constants (LECs). These parameterize (encode) the unknown high-energy (short-distance) physics and must be determined by a fit to data (or can be directly calculated if the corresponding high-energy theory is known/can be solved). The counting index \mathbf{v} in general depends on the fields in the effective theory, the number of derivatives and the number of loops. This defines the so-called power counting which allows to categorize all contributions to any matrix element at a given order. It is important to stress that \mathbf{v} must be bounded from below to define a sensible EFT. In QCD, *e.g.*, this is a consequence of the spontaneous breaking of chiral symmetry.

The contributions with the lowest possible value of \mathbf{v} define the so-called leading order (LO) contribution, the first corrections with the second smallest allowed value of \mathbf{v} the next-to-leading order (NLO) terms and so on. In contrast to more conventional perturbation theory, the small parameter is not a dimensionless coupling constant (like, *e.g.*, in Quantum Electro-

dynamics) but rather a ratio of two scales. Typically, one expands in the ratio of a small energy or momentum and the hard scale M_{hi} . A prototype of such a perturbative EFT is chiral perturbation theory that exploits the strictures of the spontaneous and explicit chiral symmetry breaking in QCD [6, 7]. Here, the light degrees of freedom are the pions, that are generated through the symmetry violation. Heavier particles like *e.g.* vector mesons only appear indirectly as they generate local four-pion interactions with four, six, etc derivatives.

In these lectures, we also consider EFTs with bound states, where certain contributions need to be resummed nonperturbatively. In section 2, we start with some general considerations. This is followed by the explicit discussion of an EFT for non-relativistic bosons with short-range interactions and large scattering length in section 3. The extension of this framework to low-energy nucleons is presented in section 4. Finally, we will discuss the inclusion of long-range interactions mediated by photon and pion exchange in 5.

2 Theoretical foundations of effective field theory

As mentioned in the introduction, effective field theories are described by writing down Lagrangians with an infinite number of terms, restricted only by symmetry considerations, and ordered by a scheme referred to as “power counting.” In this section, we discuss the meaning and importance of all these ingredients.

2.1 Top-down vs. bottom-up approaches

Generally, there are two different motivations for working with an EFT. Given a known quantum field theory, which can be solved to compute a given quantity of interest, it can be beneficial to switch to an effective description valid only in a limited energy regime simply because carrying out the calculation is more efficient with the effective theory. With such a solvable underlying theory, the parameters (“low-energy constants”) of the effective theory can be computed directly by considering some number of (simple) processes, *i.e.*, one does not need experimental input beyond what was needed to fix the parameters of the underlying theory. This approach, based on a reduction of expressions from the underlying to the effective picture is called a “top-down” approach.

An alternative procedure, somewhat closer to what we described at the outset, is to start “bottom up,” *i.e.*, by simply writing down the effective Lagrangian directly—or more precisely only those terms of the infinitely many which are needed to achieve a given desired accuracy. Being able to do that of course requires that as a first step one has already figured out which terms are allowed and how they should be ordered.

Our approach here is to work top down in the pedagogical sense, *i.e.*, postpone the discussion of the bottom-up approach and its ingredients until later in this section, and instead dive into the matter starting with examples that show how effective low-energy theories can arise from more fundamental ones. We assume that the reader is familiar with the material from a standard (relativistic) quantum field theory course.

2.1.1 Integrating out exchange particles: part I

As was also mentioned in the introduction, the very first step in the construction of an EFT is to identify the relevant degrees of freedom to work with, as well as those which are irrelevant

and thus do not need to be kept explicitly (with emphasis on the last word, because *implicitly* the physics of left-out degrees of freedom should and does enter in the effective description).

Let us illustrate this by showing how integrating out a “heavy” particle gives rise to contact interactions between the remaining degrees of freedom (see the example in section 1). We stress that the particles which are integrated out can in fact be lighter than what is left (like it is the case in pionless EFT)—what really matters for the procedure is which particles are assumed to appear in *asymptotic* states, and what is the typical energy/momentum scale between those. In that spirit, we are not making explicit assumptions about the mass hierarchy of the particles in the following. For the illustration here, we consider two scalar fields (complex and relativistic) with Yukawa interactions and start with a Lagrangian for two species:

$$\mathcal{L} = -\phi^\dagger (\square + m_\phi^2) \phi - \chi^\dagger (\square + m_\chi^2) \chi + g (\phi^\dagger \phi^\dagger \chi + \text{h.c.}) . \quad (4)$$

Suppose now we are only interested in interactions between ϕ particles at energy scales much smaller than m_χ , so that the explicit χ exchange generated by the interaction term in Eq. (4) cannot be resolved. In that case, we can derive a new effective Lagrangian that only contains ϕ degrees of freedom, a process referred to as “integrating out” the field χ stemming from its implementation in the path-integral formalism. In effect, that amounts to using the equations of motion, which we do here. From the Euler-Lagrange equation for χ^\dagger , we directly get

$$\chi = (\square + m_\chi^2)^{-1} g \phi \phi . \quad (5)$$

Defining the Klein-Gordon propagator

$$D_\chi(x-y) = \int \frac{d^4 p}{(2\pi)^4} e^{-ip(x-y)} \frac{i}{p^2 - m_\chi^2 + i\epsilon} , \quad (6)$$

satisfying

$$(\square + m_\chi^2) D_\chi(x-y) = -i\delta^{(4)}(x-y) , \quad (7)$$

we can write out Eq. (5) in configuration space as

$$\chi(x) = ig \int d^4 y D_\chi(x-y) \phi(y) \phi(y) . \quad (8)$$

Inserting this back into the Lagrangian (4), we obtain

$$\mathcal{L}(x) = -\phi^\dagger(x) (\square + m_\phi^2) \phi(x) - ig^2 \phi^\dagger(x) \phi^\dagger(x) \int d^4 y D_\chi(x-y) \phi(y) \phi(y) , \quad (9)$$

where we have written out the spacetime dependence of all fields and used Eq. (7) to cancel the terms involving $\chi^\dagger(x)$. So far, we have made only exact manipulations, but the resulting Lagrangian (9) is *non-local*, i.e., it depends on fields evaluated at different spacetime points. To simplify it further, we want to exploit the fact that χ is considered “heavy” compared to the scales we want to describe. Mathematically, this means that $D_\chi(x-y)$ is peaked at distances that are small compared to $1/m_\chi^2$. There are several ways to implement this knowledge. A particularly intuitive version is to expand the propagator (6) in momentum space,

$$\frac{i}{p^2 - m_\chi^2 + i\epsilon} = \frac{-i}{m_\chi^2} \left(1 + \frac{p^2}{m_\chi^2} + \dots \right) , \quad (10)$$

and then Fourier-transform back to configuration space. The first term gives a simple delta function, and terms with powers of p^2 induce operators with derivatives acting on $\delta(x-y)$. Inserting the leading term into Eq. (9), we arrive at the effective *local* Lagrangian

$$\mathcal{L}_{\text{eff}}(x) = -\phi^\dagger(x) (\square + m_\phi^2) \phi(x) - \frac{g^2}{m_\chi^2} \phi^\dagger(x) \phi^\dagger(x) \phi(x) \phi(x) + \dots \quad (11)$$

The ellipses contain operators with derivatives acting on $\phi(x)$, obtained from those acting on the delta functions from the propagator after integrating by parts. A diagrammatic illustration of the procedure is shown in Fig. 2.

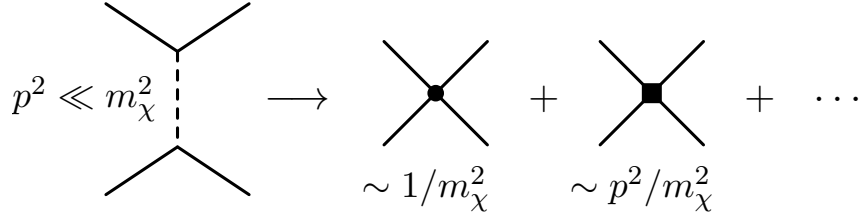


Fig. 2 Chain of contact interactions obtained by integrating out an exchange particle.

We note that an alternative derivation of the above result, discussed for example in Ref. [8], is given by Taylor-expanding the field product $\phi(y)\phi(y)$ about $y = x$ under the integral and then using the properties of the propagator. This directly gives terms with an increasing number of derivatives acting on $\phi^\dagger(x)\phi^\dagger(x)$, and those with an odd number of derivatives are found to vanish, in agreement with Eq. (10) featuring only even powers of p^2 .

2.1.2 Emergence of many-body forces

We now add a third field Φ to the Lagrangian:

$$\mathcal{L} = -\phi^\dagger (\square + m_\phi^2) \phi - \chi^\dagger (\square + m_\chi^2) \chi - \Phi^\dagger (\square + m_\Phi^2) \Phi + g (\phi^\dagger \phi^\dagger \chi + \text{h.c.}) + g' (\Phi^\dagger \phi \chi + \text{h.c.}) \quad (12)$$

The new interaction term is chosen such that Φ can “decay” into a ϕ and a χ , thus acting like a heavier version of the ϕ . In spite of the simplicity of this bosonic toy model, it is useful to think about ϕ and Φ as the nucleon and its Δ excitation, respectively, and about χ as a pion field. If we first integrate out the Φ field following the procedure described in the previous section, we find

$$\Phi(x) = ig' \int d^4y D_\Phi(x-y) \phi(y) \chi(y), \quad (13)$$

and thus

$$\mathcal{L}_{\text{eff}} = -\phi^\dagger (\square + m_\phi^2) \phi - \chi^\dagger (\square + m_\chi^2) \chi + g (\phi^\dagger \phi^\dagger \chi + \text{h.c.}) + \frac{g'^2}{m_\Phi^2} \phi^\dagger \chi^\dagger \phi \chi + \dots, \quad (14)$$

where we have only kept the leading (no derivatives) induced contact interaction. Proceeding as before for the χ field, we now get

$$(\square + m_\chi^2) \chi = g \phi \phi + \frac{g'^2}{m_\Phi^2} \phi^\dagger \phi \chi + \dots \quad (15)$$

This can no longer be solved exactly because we now have a χ on the right-hand side. However, using the general operator identity

$$(\hat{A} - \hat{B})^{-1} = \hat{A}^{-1} + \hat{A}^{-1} \hat{B} \hat{A}^{-1} + \dots, \quad (16)$$

we can write down a formal iterative solution:

$$\chi = \left(\square + m_\chi^2\right)^{-1} g\phi\phi + \left(\square + m_\chi^2\right)^{-1} \frac{g'^2}{m_\phi^2} \phi^\dagger \phi \left(\square + m_\chi^2\right)^{-1} g\phi\phi + \dots, \quad (17)$$

with each of the inverse differential operators giving a propagator when written out. Those, in turn, each give factors of $-i/m_\phi^2$ times a delta function, plus additional terms with derivatives.

1. Exercise: Derive Eq. (16).

Inserting the above result back into the Eq. (14), we see that in addition to the two-body contact operator $(\phi^\dagger \phi)^2$ obtained previously, we now also get all kinds of higher-body interactions. For example, we get a three-body force through

$$\frac{g'^2}{m_\phi^2} \phi^\dagger \chi^\dagger \phi \chi \rightarrow \frac{g'^2 g^2}{m_\phi^2 m_\chi^4} (\phi^\dagger \phi)^3. \quad (18)$$

In Fig. 3 it is illustrated diagrammatically how such a term arises subsequently, starting from a diagram derived from the original Lagrangian (12) with three fields.

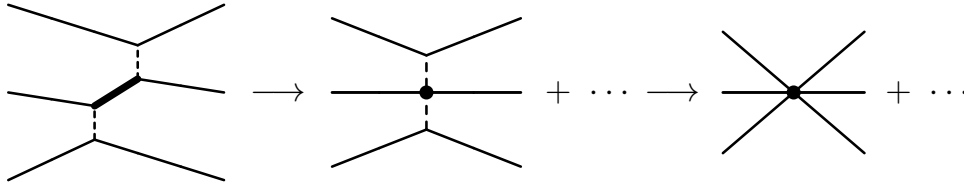


Fig. 3 Emergence of a three-body contact interaction.

2.2 Nonrelativistic field theory

Relativistic effects and exact Lorentz invariance are not crucial to describe systems at low energies, where “low” means “much smaller than the particles’ rest mass.” Based on that, one typically starts with a nonrelativistic framework and writes down effective Lagrangians of so-called Schrödinger fields, *e.g.*,

$$\mathcal{L}_{\phi, \text{free}} = \phi^\dagger \left(i\partial_t + \frac{\nabla^2}{2m} \right) \phi \quad (19)$$

for a free scalar particle, where $\phi^\dagger(t, \mathbf{x})$ is the field operator that creates a particle at time t and position \mathbf{x} , and $\phi(t, \mathbf{x})$ correspondingly destroys it. Written in terms of momentum-space ladder operators $\hat{a}_{\mathbf{p}}, \hat{a}_{\mathbf{p}}^\dagger$ (as they appear in standard many-body quantum mechanics), we have

$$\phi(t, \mathbf{x}) = \int \frac{d^3 p}{(2\pi)^3} \hat{a}_{\mathbf{p}} e^{-iE_{\mathbf{p}} t} e^{i\mathbf{p} \cdot \mathbf{x}}, \quad (20)$$

and analogously for $\phi^\dagger(t, \mathbf{x})$. Note that here $E_{\mathbf{p}} = \mathbf{p}^2/(2m)$ is the kinetic energy alone, and that creation and destruction operators are completely separated. Intuitively, this makes perfect sense: At low energies, virtual particle-antiparticle pairs would be highly off-shell, thus giving rise to very short-range effects that we can simply describe as contact interactions. Other effects, such as self-energy corrections to the particle mass, are automatically accounted for by

using the physical value for m in Eq. (19). With this in mind, one can proceed in the bottom-up approach and construct an interacting theory by supplementing the free Lagrangian with all allowed contact operators. In particular, like Eq. (19) they should all be invariant under Galilei transformations, the low-energy remnant of the Poincaré group. Before we come back to this, however, we find it instructive to explicitly consider the low-energy limit of a relativistic theory.

2.2.1 Nonrelativistic limit of a bosonic field

Let us make the connection of Eq. (19) to a relativistic complex Klein–Gordon field Φ , the Lagrangian for which can be written as

$$\mathcal{L}_{\Phi,\text{free}} = -\Phi^\dagger \left(\partial_t^2 - \nabla^2 + m^2 \right) \Phi. \quad (21)$$

Using integration by parts, this can be shown to be equivalent to the more common form written with $(\partial_\mu \Phi^\dagger)(\partial^\mu \Phi)$. This implies the Klein–Gordon equation for the field operator,

$$\left(\partial_t^2 - \nabla^2 + m^2 \right) \Phi = 0, \quad (22)$$

the most general solution of which is typically written as (with a four-vectors $x = (t, \mathbf{x})$, $p = (p_0, \mathbf{p})$, and a Lorentz-invariant integration measure)

$$\Phi(x) = \int \frac{d^3p}{(2\pi)^3} \frac{1}{\sqrt{2\omega_{\mathbf{p}}}} \left(\hat{a}_{\mathbf{p}} e^{-ip \cdot x} + \hat{b}_{\mathbf{p}}^\dagger e^{ip \cdot x} \right) \Big|_{p_0=\omega_{\mathbf{p}}}, \quad (23)$$

where $\omega_{\mathbf{p}} = \sqrt{\mathbf{p}^2 + m^2}$. With this convention where p_0 is chosen positive, modes created by $\hat{a}_{\mathbf{p}}^\dagger$ correspond to particles (propagating forward in time), whereas $\hat{b}_{\mathbf{p}}^\dagger$ creates an antiparticle (positive-energy state propagating backwards in time). That we have both stems from the fact that the complex scalar field corresponds to two real ones (completely decoupled in the absence of interactions), each of which comes with its own pair of creation and annihilation operators. To take the nonrelativistic limit, we have to consider the particle and antiparticles separately. Defining

$$\phi_a(x) = \int \frac{d^3p}{(2\pi)^3} \frac{1}{\sqrt{2\omega_{\mathbf{p}}}} \hat{a}_{\mathbf{p}} e^{-ip \cdot x} \Big|_{p_0=\omega_{\mathbf{p}}} \equiv e^{-imt} \phi_a(x), \quad (24)$$

and plugging this into the Klein–Gordon equation, we get

$$e^{-imt} \left[\partial_t^2 - 2im \partial_t - \nabla^2 \right] \phi_a(x) = 0, \quad (25)$$

where the quadratic mass term has canceled. Since $\phi_a(x) = e^{imt} \phi_a(x)$, we see from Eq. (24) that in the Fourier transform each time derivative acting on $\phi_a(x)$ brings down a factor

$$\omega_p - m = \sqrt{\mathbf{p}^2 + m^2} - m \approx \mathbf{p}^2/(2m), \quad (26)$$

i.e., just the kinetic energy $E_{\mathbf{p}}$ up to corrections of higher order in $1/m$. In the nonrelativistic limit, $E_{\mathbf{p}} \ll m$, so we see that we can neglect the quadratic time derivative in Eq. (25) compared to the other two terms in Eq. (25), and then recover the Schrödinger equation for ϕ_a :

$$\left(i\partial_t + \frac{\nabla^2}{2m}\right)\phi_a(x) = 0. \quad (27)$$

This establishes the connection to our $\phi(t, \mathbf{x})$ in Eq. (19) when we insert an additional factor $\sqrt{2m}$ in the field redefinition to account for the otherwise different normalizations. For the antiparticles, we can carry out an analogous procedure, except that we have to choose the opposite sign for the mass-dependent phase in the field redefinition analogous to Eq. (24) because the antiparticle part of $\varphi(x)$ comes with a factor $e^{+ip \cdot x}$.

2.2.2 Nonrelativistic fermions

For relativistic Dirac fermions, the nonrelativistic reduction can be carried out with the help of a so-called Foldy-Wouthuysen transformation.³ The idea behind the approach is to decouple the particle and antiparticle modes contained together in a four-spinor ψ through a sequence of unitary transformations. In the following, we demonstrate this procedure, using an *interacting* model theory to also illustrate what happens to interaction terms in the nonrelativistic limit. Since it will be useful to motivate the pionless EFT discussed in Sec. 4, we start with a Lagrangian of the form

$$\begin{aligned} \mathcal{L} = \bar{\psi} (i\partial - M_N) \psi + \frac{1}{2}(\partial^\mu \vec{\pi}) \cdot (\partial_\mu \vec{\pi}) - \frac{1}{2}m_\pi^2 \vec{\pi}^2 + \frac{1}{2}(\partial^\mu \sigma) \cdot (\partial_\mu \sigma) - \frac{1}{2}m_\sigma^2 \sigma^2 \\ - g \bar{\psi} (\sigma - i\gamma^5 \vec{\tau} \cdot \vec{\pi}) \psi, \end{aligned} \quad (28)$$

where the nucleon field ψ is an isospin doublet of Dirac spinors, π is an isospin triplet, and σ is an isoscalar. A Lagrangian of this form (plus additional interaction terms among σ and π), can be obtained from a linear sigma model after spontaneous symmetry breaking (see, for example, [8], Chapter I) and augmented by an explicit mass term for π .⁴ We denote the Pauli matrices in spin and isospin space as $\sigma = (\sigma^i)$ and $\tau = (\tau^\lambda)$, respectively. For the gamma matrices we use the standard (Dirac) representation:

$$\gamma^0 = \begin{pmatrix} \mathbf{1} & 0 \\ 0 & -\mathbf{1} \end{pmatrix}, \quad \gamma^i = \begin{pmatrix} 0 & \sigma^i \\ -\sigma^i & 0 \end{pmatrix}, \quad \gamma^5 = \begin{pmatrix} 0 & \mathbf{1} \\ \mathbf{1} & 0 \end{pmatrix}. \quad (29)$$

To perform the nonrelativistic reduction, we start by separating odd and even operators, which are two-by-two block matrices in Dirac space. The result is

$$\mathcal{L}_\psi = \psi^\dagger (\hat{E} + \hat{O} - \gamma^0 M_N) \psi, \quad (30)$$

where

$$\hat{E} = \begin{pmatrix} i\partial_t - g\sigma & 0 \\ 0 & i\partial_t + g\sigma \end{pmatrix} \quad \text{and} \quad \hat{O} = \begin{pmatrix} 0 & -i\vec{\sigma} \cdot \nabla + ig\vec{\tau} \cdot \vec{\pi} \\ -i\vec{\sigma} \cdot \nabla - ig\vec{\tau} \cdot \vec{\pi} & 0 \end{pmatrix}. \quad (31)$$

Rotating the phase of the fermion field,

$$\psi \rightarrow \tilde{\psi} = e^{-iM_N t} \psi, \quad (32)$$

just like we did for the bosonic field in Eq. (24), we can remove the mass term for the upper components:

$$\mathcal{L}_\psi = \tilde{\psi}^\dagger (\hat{E} + \hat{O} - (\gamma^0 - \mathbf{1})M_N) \tilde{\psi}. \quad (33)$$

³ An alternative way to perform the nonrelativistic reduction is to introduce a “heavy fermion” field [9]. A comparison of this formalism and the Foldy-Wouthuysen transformation can be found in Ref. [10].

⁴ We stress, however, that this really is a model and not a proper EFT describing QCD.

The Foldy-Wouthuysen transformation is now constructed to (approximately) decouple the upper from the lower components, *i.e.*, nucleons from their antiparticles. To achieve this, we use a sequence of further unitary redefinitions of the fermion field. The first of these is

$$\tilde{\psi} \rightarrow \tilde{\psi}' = e^{-i\hat{S}} \tilde{\psi} \quad \text{with} \quad \hat{S} = -\frac{i\gamma^0 \hat{O}}{2M_N}. \quad (34)$$

Let us consider this transformation up to quadratic order in $1/M_N$. Expanding the exponential, we have

$$\tilde{\psi} = e^{i\hat{S}} \tilde{\psi}' = \left(1 + \frac{\gamma^0 \hat{O}}{2M_N} + \frac{(\gamma^0 \hat{O})^2}{8M_N^2} + \mathcal{O}(1/M_N^3) \right) \tilde{\psi}' \quad (35)$$

and likewise

$$\tilde{\psi}^\dagger = \tilde{\psi}'^\dagger e^{-i\hat{S}} = \tilde{\psi}'^\dagger \left(1 - \frac{\gamma^0 \hat{O}}{2M_N} + \frac{(\gamma^0 \hat{O})^2}{8M_N^2} + \mathcal{O}(1/M_N^3) \right). \quad (36)$$

Inserting this into Eq. (33) and collecting contributions up to corrections which are $\mathcal{O}(1/M_N^2)$, we get a number of terms:

$$-\frac{\gamma^0 \hat{O} \hat{E}}{2M_N} + \frac{\hat{E} \gamma^0 \hat{O}}{2M_N} = \frac{\gamma^0 [\hat{O}, \hat{E}]}{2M_N} \quad (37a)$$

$$\frac{\hat{O} \gamma^0 \hat{O}}{2M_N} - (\gamma^0 - \mathbf{1}) \frac{(\gamma^0 \hat{O})^2}{8M_N} - \frac{\gamma^0 \hat{O}^2}{2M_N} + \frac{\gamma^0 \hat{O}}{2M_N} (\gamma^0 - \mathbf{1}) \frac{\gamma^0 \hat{O}}{2M_N} - \frac{(\gamma^0 \hat{O})^2}{8M_N} (\gamma^0 - \mathbf{1}) = -\frac{\gamma^0 \hat{O}^2}{2M_N}, \quad (37b)$$

$$\frac{1}{2} \gamma^0 \hat{O} (\gamma^0 - \mathbf{1}) - \frac{1}{2} (\gamma^0 - \mathbf{1}) \gamma^0 \hat{O} = -\hat{O}. \quad (37c)$$

Above we have used that

$$[\gamma_0, \hat{E}] = 0, \quad \{\gamma_0, \hat{O}\} = 0, \quad (38)$$

and $(\gamma^0)^2 = \mathbf{1}$. Collecting everything, we get

$$\mathcal{L}_\psi = \tilde{\psi}'^\dagger \left(\hat{E} - \frac{\gamma^0 \hat{O}^2}{2M_N} + \frac{\gamma^0 [\hat{O}, \hat{E}]}{2M_N} - (\gamma^0 - \mathbf{1}) M_N \right) \tilde{\psi}' + \mathcal{O}(1/M_N^2). \quad (39)$$

The \hat{O}^2 term is even and we see that the original odd operator is canceled, but we have generated a new term $\sim [\hat{O}, \hat{E}]$. If we neglect the interaction and consider

$$\hat{E} = \hat{E}_{\text{free}} = \begin{pmatrix} i\partial_t & 0 \\ 0 & i\partial_t \end{pmatrix} \quad \text{and} \quad \hat{O} = \hat{O}_{\text{free}} = \begin{pmatrix} 0 & -i\boldsymbol{\sigma} \cdot \boldsymbol{\nabla} \\ -i\boldsymbol{\sigma} \cdot \boldsymbol{\nabla} & 0 \end{pmatrix}, \quad (40)$$

we find that $[\hat{O}_{\text{free}}, \hat{E}_{\text{free}}] = 0$ (partial derivatives commute) and thus the desired decoupling up to $\mathcal{O}(1/M_N^2)$. For the interacting case, on the other hand, the commutator does not vanish. We see, however, that the new odd contribution is suppressed by a factor $1/M_N$. To push it to the next higher order, we need another rotation:

$$\tilde{\psi}' \rightarrow \tilde{\psi}'' = e^{-i\hat{S}'} \tilde{\psi}', \quad (41a)$$

with

$$\hat{S}' = -\frac{i\gamma^0 \hat{O}'}{2M_N} \quad \text{with} \quad \hat{O}' = \frac{\gamma^0 [\hat{O}, \hat{E}]}{2M_N} \quad (41b)$$

After a couple of steps, we arrive at

$$\mathcal{L}_\psi = \tilde{\psi}''^\dagger \left(\hat{E} - \frac{\gamma^0 \hat{O}^2}{2M_N} - (\gamma^0 - \mathbf{1}) M_N \right) \tilde{\psi}'' + \mathcal{O}(1/M_N^2), \quad (42)$$

i.e., up to $\mathcal{O}(1/M_N^2)$ there are now no odd terms left and the upper and lower components of $\tilde{\psi}''$ are decoupled at this order.

2. Exercise: Carry out the steps that lead from the transformation (41) to Eq. (42). Note that it suffices to expand the exponentials up to first order.

In this Lagrangian, we can now write

$$\tilde{\psi}'' = \begin{pmatrix} N \\ n \end{pmatrix} \quad (43)$$

and identify the upper (“large”) component N —a doublet in both spin and isospin space—with the particle and the lower (“small”) component with the antiparticle states. The term $(\gamma^0 - \mathbf{1})M_N$ in Eq. (42) ensures that there is no explicit mass term for the field N , whereas that for n comes with a factor two, corresponding to the Dirac mass gap between particles and antiparticles. Let us now write down the Lagrangian obtained for N , omitting the decoupled small components:

$$\mathcal{L}_\psi = N^\dagger \left(i\partial_t - g\sigma - \frac{1}{2M_N} [-i\vec{\sigma} \cdot \nabla + ig\vec{\tau} \cdot \vec{\pi}] [-i\vec{\sigma} \cdot \nabla - ig\vec{\tau} \cdot \vec{\pi}] \right) N + \dots \quad (44)$$

To simplify this further, we use that⁵

$$(\vec{\sigma} \cdot \nabla)(\vec{\sigma} \cdot \nabla) = \nabla^2 \quad (45)$$

and, from the product rule,

$$(\vec{\sigma} \cdot \nabla)(\vec{\tau} \cdot \vec{\pi}) = \vec{\sigma} \cdot (\vec{\tau} \cdot \nabla \vec{\pi}) + (\vec{\tau} \cdot \vec{\pi})(\vec{\sigma} \cdot \nabla) = \sigma^i \tau^a (\partial_i \pi^a) + \tau^a \pi^a \sigma^i \partial_i. \quad (46)$$

In the last step we have written out all indices to clarify the meaning of the two dot products. Collecting everything, we find that the $(\vec{\tau} \cdot \vec{\pi})(\vec{\sigma} \cdot \nabla)$ terms cancel out and arrive at

$$\begin{aligned} \mathcal{L} = N^\dagger \left(i\partial_t + \frac{\nabla^2}{2M_N} \right) N - g\sigma N^\dagger N + N^\dagger \left(\frac{g}{2M_N} \vec{\sigma} \cdot (\vec{\tau} \cdot \nabla \vec{\pi}) + \frac{g^2}{2M_N} (\vec{\tau} \cdot \vec{\pi})^2 \right) N \\ + \frac{1}{2} (\partial^\mu \vec{\pi}) \cdot (\partial_\mu \vec{\pi}) - \frac{1}{2} m_\pi^2 \vec{\pi}^2 + \frac{1}{2} (\partial^\mu \sigma) \cdot (\partial_\mu \sigma) - \frac{1}{2} m_\sigma^2 \sigma^2 + \dots \end{aligned} \quad (47)$$

This includes the expected nonrelativistic kinetic term for the fermion field, as well as various interactions with σ and $\vec{\pi}$. Note that the latter two particles are still relativistic and unchanged by the Foldy-Wouthuysen transformation, so that we could simply reinstate their kinetic terms as in Eq. (28).

2.2.3 Integrating out exchange particles: part II

With Eq. (28) we are now also in a convention situation to illustrate how we end up with only contact interactions between the nonrelativistic fermions if we integrate out the σ and $\vec{\pi}$ fields. Their equations of motion are

$$(\square + m_\sigma^2) \sigma = gN^\dagger N \quad (48)$$

⁵ Note that Eq. (45) is very simple because we have not included a coupling of ψ to the electromagnetic field. If we had done that, the ∇ would be a covariant derivative, $\mathbf{D} = \nabla + ie\mathbf{A}$, and Eq. (45) would generate, among other terms, the magnetic spin coupling $\vec{\sigma} \cdot \mathbf{B}$.

and

$$(\square + m_\pi^2) \pi^\lambda = -\frac{g}{2M_N} \nabla \cdot [N^\dagger \vec{\sigma} \tau^\lambda N] - \frac{g^2}{M_N} N^\dagger (\vec{\tau} \cdot \vec{\pi}) \tau^\lambda N. \quad (49)$$

The σ part can be handled exactly as in Sec. 2.1.1, giving a leading four-nucleon contact interaction $\sim g^2/m_\sigma^2$ plus a tower of operators with increasing number of derivatives. The $\vec{\pi}$ part is more interesting, but also more complicated due to the derivative in Eq. (49). We thus keep the following discussion rather qualitative and leave it as an exercise to work out the details.

In that spirit, we consider only the first term in Eq. (49), corresponding to a one- $\vec{\pi}$ -exchange operator when substituted back into the Lagrangian. With the propagator $D_\pi(x-y)$ defined in complete analogy to Eq. (6), we can write

$$\pi^\lambda(x) = -\frac{ig}{2M_N} \int d^4y D_\pi(x-y) \partial_j^y [N^\dagger(y) \sigma^j \tau^\lambda N(y)] + \dots, \quad (50)$$

and thus get

$$\mathcal{L}_{\text{int}} \sim [N^\dagger(x) \sigma^i \tau^\lambda N(x)] \partial_i^x \int d^4y D_\pi(x-y) \partial_j^y [N^\dagger(y) \sigma^j \tau^\lambda N(y)] + \dots, \quad (51)$$

where for the time being we omit the prefactor $g^2/(4M_N^2)$. We integrate by parts to have ∂_j^y act on $D_\pi(x-y)$. The ∂_i^x does this already, so, with all indices written out for clarity:

$$\mathcal{L}_{\text{int}} \sim \int d^4y N_{aa}^\dagger(x) (\sigma^i)^\alpha_\beta (\tau^\lambda)^a_b N^{\beta b}(x) [\partial_x^i \partial_y^j D_\pi(x-y)] N_{\gamma c}^\dagger(y) (\sigma^j)^\gamma_\delta (\tau^\lambda)^c_d N^{\delta d}(y) + \dots. \quad (52)$$

From the definition of the propagator we find that

$$\partial_i^x \partial_j^y D_\pi(x-y) = \int \frac{d^4p}{(2\pi)^4} (ip_i)(-ip_j) e^{-ip(x-y)} \frac{i}{p^2 - m_\pi^2 + i\epsilon} = -\partial_i^x \partial_j^x D_\pi(x-y), \quad (53)$$

so the partial derivatives can be written fully symmetric in i and j . The various fermion field operators can be rearranged with the help of

$$\begin{aligned} N^{\beta b}(x) N_{\gamma c}^\dagger(y) = & -\frac{1}{4} \left[(N^\dagger(y) N(x)) \delta_\gamma^\beta \delta_c^b + (N^\dagger(y) \tau^\kappa N(x)) \delta_\gamma^\beta (\tau^\kappa)^b_c \right. \\ & \left. + (N^\dagger(y) \sigma^k N(x)) (\sigma^k)^\beta_\gamma \delta_c^b + (N^\dagger(y) \tau^\kappa \sigma^k N(x)) (\sigma^k)^\beta_\gamma (\tau^\kappa)^b_c \right]. \end{aligned} \quad (54)$$

Using also

$$\sigma^i \sigma^j = \delta^{ij} \mathbf{1} + i\epsilon^{ijk} \sigma^k, \quad (55a)$$

$$\sigma^i \sigma^k \sigma^j = \delta^{kj} \sigma^i + \delta^{ki} \sigma^j - \delta^{ij} \sigma^k + i\epsilon^{ikj} \mathbf{1}, \quad (55b)$$

$$\sigma^i \sigma^j \sigma^i = -\sigma^j, \quad (55c)$$

we get four terms from Eq. (52) decomposed into contributions symmetric and antisymmetric in i and j , with the latter all vanishing upon contraction with $\partial_i^x \partial_j^x$. The simplest symmetric term comes with a δ^{ij} , yielding $\nabla^2 D_\pi(x-y)$. To see what this generates, we Taylor-expand the fermion fields that depend on y about x , e.g., $N(y) = N(x) + (y-x)^\mu \partial_\mu N(x) + \dots$. This gives as the leading piece a combination of four fermion operators all evaluated at x , times

$$\int d^4y \int \frac{d^4p}{(2\pi)^4} e^{-ip \cdot (x-y)} \frac{ip^2}{p^2 - m_\pi^2 + i\epsilon} = \int d^4y \int \frac{d^3p}{(3\pi)^4} \int \frac{dp_0}{2\pi} e^{-ip(x-y)} \frac{ip^2}{p_0^2 - \mathbf{p}^2 - m_\pi^2 + i\epsilon}. \quad (56)$$

The integral over p_0 can be solved via contour integration. Defining $\omega_{\mathbf{p}} = \sqrt{\mathbf{p}^2 + m_\pi^2}$, we get

$$\int \frac{dp_0}{2\pi} e^{-ip_0(x_0-y_0)} \frac{i}{p_0^2 - \mathbf{p}^2 - m_\pi^2 + i\varepsilon} = \frac{e^{-i\omega'_\mathbf{p}|x_0-y_0|}}{2\omega'_\mathbf{p}} \quad \text{with} \quad \omega'_\mathbf{p} = \omega_\mathbf{p} - \frac{i\varepsilon}{2\omega_\mathbf{p}} \equiv \omega_\mathbf{p} - i\varepsilon'. \quad (57)$$

It is important here to keep track of the small imaginary part, as it allows us to write

$$\int_{-\infty}^{\infty} dy_0 \frac{e^{-i\omega'_\mathbf{p}|x_0-y_0|}}{2\omega'_\mathbf{p}} = \int_0^{\infty} dy_0 \frac{e^{-i\omega'_\mathbf{p}|y_0|}}{\omega'_\mathbf{p}} = -i/(\omega'_\mathbf{p})^2. \quad (58)$$

Collecting the results up to this point, we arrive at

$$\int d^4y \int \frac{d^4p}{(2\pi)^4} e^{-ip(x-y)} \frac{i\mathbf{p}^2}{p^2 - m_\pi^2 + i\varepsilon} = - \int d^3y \int \frac{d^3p}{(2\pi)^3} e^{i\mathbf{p}\cdot(\mathbf{x}-\mathbf{y})} \frac{\mathbf{p}^2}{p^2 + m_\pi^2}. \quad (59)$$

We finally obtain the desired contact interaction by expanding

$$\frac{\mathbf{p}^2}{p^2 + m_\pi^2} = \frac{\mathbf{p}^2}{m_\pi^2} \left(1 - \frac{\mathbf{p}^2}{m_\pi^2} + \dots \right), \quad (60)$$

with a leading term $\sim \mathbf{p}^2$, generating a contact interaction $\sim (N^\dagger N) \nabla^2 (N^\dagger N)$. This is of course not surprising: after all, the original interaction term in Eq. (47) generating the contact operator had a single derivative ∇ . Considering other terms coming from Eq. (54), one can also find operators like $(N^\dagger \vec{\sigma} \cdot \nabla N)(N^\dagger \vec{\sigma} \cdot \nabla N)$, and it is a useful exercise to work this out in detail. But already from our qualitative discussion here we can infer that the resulting effective theory is an expansion in \mathbf{p}^2/m_π^2 , *i.e.*, its range of validity is determined by three-momenta—rather than the energies—being small compared to m_π .⁶

2.2.4 The Schrödinger field

We conclude this section by looking at the non-relativistic field theory from a more general perspective, establishing its close connection to the “second quantized” approach to (many-body) quantum mechanics that is used in several later chapters of this volume.

Recall from the beginning of this section that the Lagrangian (19) for the free Schrödinger field ϕ is

$$\mathcal{L}_{\phi,\text{free}} = \phi^\dagger \left(i\partial_t + \frac{\nabla^2}{2m} \right) \phi. \quad (61)$$

This trivially gives the equation of motion

$$\left(i\partial_t + \frac{\nabla^2}{2m} \right) \phi = 0, \quad (62)$$

which is formally the same as the free Schrödinger equation. However, recall that ϕ here is a field *operator*, *i.e.*, $\phi(x)$ creates a particle at $x = (t, \mathbf{x})$ from the vacuum, so to really get an ordinary Schrödinger equation, we have to act with both sides of Eq. (62) on $|0\rangle$, and define the quantum-mechanical one-body state

$$|\phi(t, \mathbf{x})\rangle = \phi(t, \mathbf{x}) |0\rangle. \quad (63)$$

If we add to Eq. (61) a term $V(x)\phi^\dagger(x)\phi(x)$, we obtain the Schrödinger equation for a particle in a potential $V(x)$. Exactly as for a relativistic field we can define the propagator

⁶ This is assuming $m_\pi < m_\sigma$.

$$D_\phi(x-y) = \int \frac{d^4 q}{(2\pi)^4} e^{-ip(x-y)} \frac{i}{p_0 - \frac{\mathbf{p}^2}{2m} + i\epsilon}, \quad (64)$$

satisfying

$$\left(i\partial_t + \frac{\nabla^2}{2m}\right) D_\phi(x-y) = -i\delta^{(4)}(x-y). \quad (65)$$

Up to a conventional factor i , this is precisely the (retarded) Green's function⁷ familiar, for example, from non-relativistic scattering theory (then typically denoted G_0). This will appear again when the Lippmann–Schwinger equation is derived using the field-theory language in Sec. 3.

While it is nice and reassuring that we can go back to simple quantum mechanics from the one-body Schrödinger Lagrangian discussed so far, this feature is not very relevant in practice. We can, however, straightforwardly generalize it to the many-body case. To that end, consider a Lagrangian that includes a two-body interaction, written in terms of a general non-local potential:⁸

$$\mathcal{L}_{\phi,2\text{-body}}(x) = \phi^\dagger(x) \left(i\partial_t + \frac{\nabla^2}{2m}\right) \phi(x) + \int d^4 y \phi^\dagger(x) \phi(x) V(x,y) \phi^\dagger(y) \phi(y). \quad (66)$$

Note that this has exactly the structure that we found when we integrated out particles in the preceding sections, before expanding the propagators to get simple contact interactions. Such a Lagrangian (possibly including also higher-body forces) is a convenient starting point for example for many-body perturbation theory used to study quantum systems at finite density.

Coming back to effective field theories, we stress that these are *not* defined by putting a given potential into a Lagrangian; in doing that, one merely gets a model written in a convenient way. The EFT instead makes no assumptions on the interaction (besides symmetry constraints). It is thus much more general and not a model, but to be predictive it requires a number of *a priori* unknown parameters to be fixed and its various terms to be ordered systematically. It is this that we turn to next.

2.3 Symmetries and power counting

So far, we have discussed how to obtain effective low-energy Lagrangians by integrating out "heavy" degrees of freedom, leaving only those that we want to describe at low energies or rather, as we showed explicitly with the pseudoscalar pion-nucleon model, low momenta. We found the contact interactions generated this way to come with the integrated-out particle's mass in the denominator, and with an increasing number of derivatives as we keep more and more terms from the expansion. These derivatives will turn into powers of momentum, which is a small scale for external states. We furthermore showed how a nonrelativistic reduction generates a chain of operators with an increasing power of the particle's mass in the denominator, thus also giving a hierarchy of terms that eventually restore the original theory's relativistic structure with coupling between particles and antiparticles.

⁷ Note that in the nonrelativistic case there is no "Feynman propagator." Particles and antiparticles are decoupled, and the denominator in Eq. (64) only has a single pole at $p_0 = \mathbf{p}^2/(2m) - i\epsilon$. Flipping the sign of the $i\epsilon$ term gives the advanced Green's function.

⁸ A static (time-independent) potential, as it is more common in quantum mechanics, would be a function only of \mathbf{x} and \mathbf{y} , and all fields in the interaction term would be evaluated at the same time t .

From these procedures it is clear that the terms in the effective Lagrangian should be ordered in a natural way, with the most important ones being those with the least number of large mass scales in the denominator and the least number of derivatives in the numerator. It is also clear that they are restricted in their structure. For example, if we start with a Lorentz-invariant relativistic theory, after the nonrelativistic reduction we will only get terms that are invariant under “small” Lorentz boosts. More precisely, the nonrelativistic operators should be invariant under Galilean transformations (assuming the original theory had rotational invariance, this simply gets inherited by the effective one), and the form of so-called “relativistic corrections” is determined by the expansion of the dispersion relation for positive-energy solutions:

$$E = \sqrt{m^2 + p^2} = m + \frac{p^2}{2m} - \frac{p^4}{8m^3} + \dots \quad (67)$$

We now turn to discussing the bottom-up approach guided by these principles. To that end, consider the effective Lagrangian for a nonrelativistic bosonic field with contact interactions:

$$\begin{aligned} \mathcal{L} = & \phi^\dagger \left(i\partial_t + \frac{\nabla^2}{2m} \right) \phi + \phi^\dagger \frac{\nabla^4}{8m^3} \phi + \dots \\ & + g_2^{(0)} (\phi^\dagger \phi)^2 + g_2^{(2s/p)} \left((\phi^\dagger \overleftrightarrow{\nabla} \phi)^2 - (\phi^\dagger \phi) (\phi^\dagger (\overleftrightarrow{\nabla})^2 \phi) \mp 2(\phi^\dagger \phi) \nabla^2 (\phi^\dagger \phi) \right) + \dots \\ & + g_3^{(0)} (\phi^\dagger \phi)^3 + \dots \end{aligned} \quad (68)$$

Here we have used the definition

$$f \overleftrightarrow{\nabla} g = f(\nabla)g - (\nabla f)g \quad (69)$$

and conveniently separated the two-body terms with two derivatives into those which contribute to S-wave ($\sim g_2^{(2s)}$) and P-wave ($\sim g_2^{(2p)}$) interactions, respectively. One can of course choose different linear combinations, but a separation by partial waves is typically a good choice for systems with rotational invariance. It is a useful exercise to work out how the structure for the derivative interactions gives the desired result, working in momentum space and considering contractions with external in and out states that have center-of-mass momenta $\pm \mathbf{k}^2$ and $\pm \mathbf{p}/2$, respectively. The structure of the individual terms is determined by the requirement of Galilean invariance,⁹ and the EFT paradigm tells us to write down all possible terms with a given number of derivatives (with odd numbers excluded by parity invariance).

2.3.1 The breakdown scale

As mentioned in the introduction, the most important requirement to construct an EFT is the identification of—at least two, but possibly more—separated scales, ratios of which are used to extract a small expansion parameter. The better the scale separation, the smaller this parameter becomes, and consequently the better the more precise (and, provided all contributions have been identified correctly, accurate) the theory becomes at any given order in the expansion. In the simplest case, there is one low scale Q associated with the typical momentum of the physical system that we want to describe, and a single large scale M_{hi} , the “breakdown scale” associated with the physics that our EFT does not take into account—in other words: resolve—explicitly. This is exactly the situation that we constructed when we integrated out exchange particles from a given theory in Secs. 2.1.1 and 2.2.3. By construction,

⁹ See for example Ref. [11], Sec. 2.1.1 for a rigorous discussion of the required transformation properties.

the EFT is not appropriate to describe processes with momenta of the order of or large than the breakdown scale. To emphasize this meaning, it is sometimes also denoted by the letter Λ (with or possibly without some qualifying subscript).¹⁰

As already mentioned, integrating out degrees of freedom from a given more fundamental theory will naturally give a breakdown scale set by that particle’s mass. But it can also be something more general. For example, although in the situations discussed here so far the particles we were ultimately interested in were already present as degrees of freedom in the original theory, such a scenario is merely a special case. The first step in writing down an effective field theory is to identify what the appropriate—literally: effective—degrees of freedom are for the processes one wants to describe, and they can be different from those of the fundamental theory. This is exactly the case in nuclear physics: while the degrees of freedom in quantum chromodynamics (QCD) are quarks and gluons, describing the binding of nuclei with these is, although possible with state-of-the-art lattice QCD calculations, largely inefficient to say the least. It is much more economical to work with nucleons directly as degrees of freedom, as done in most chapters of this volume, because a detailed knowledge of the internal structure of protons and neutrons is not necessary to describe their binding into nuclei; it is only resolved at much higher energies, for example in deep inelastic scattering. The reason for this is color confinement: the low-energy degrees of freedom of QCD are not quarks and gluons, but color-neutral hadrons. Chiral effective field theory, which we will come back to in Sec. 5.3, is designed to work at momenta of the order of pion mass, breaking down at the scale of chiral-symmetry breaking (estimated to be roughly a GeV, but possibly lower).

Other examples are halo EFT, constructed to describe nuclear systems that have the structure of a few nucleons weakly bound to a tight core, which can then effectively be treated as a structureless particle. Clearly, such a theory will break down at momenta large enough to probe the core’s internal structure. Similarly, one can construct an effective theory for systems of ultracold atomic gases, the constituents of which can be treated as pointlike degrees of freedom without using QED to describe their individual structure, and much less QCD to describe their atomic nuclei.

Whatever the breakdown scale is, once identified it can be used to systematically order terms in the effective Lagrangian by powers of $Q/M_{\text{hi}} \ll 1$, and we now turn to discussing how this ordering can be set up.

2.3.2 Naïve dimensional analysis

In our units with $\hbar = c = 1$, the action

$$S = \int d^4x \mathcal{L}(x) \quad (70)$$

has to be a dimensionless quantity. This, in turn, fixes the dimensions for the individual building blocks in the Lagrangian. In a relativistic theory, mass and energy are equivalent and one would simply express everything in terms of a generic mass dimension. For our nonrelativistic framework, on the other hand, energies are *kinetic* energies because the time dependence associated with the rest mass has been absorbed into the field (*cf.* Secs. 2.2.1 and 2.2.2). This implies that energy and mass scales—as well as time and space—should be counted sepa-

¹⁰ We alert the reader that in the literature this is sometimes referred to as the “cutoff of the EFT.” We do not use that language to avoid confusion with an (arbitrary) momentum cutoff introduced to regularize divergent loop integrals (discussed).

rately.¹¹ In fact, it is more natural to consider powers of momentum. To understand what this means, let us start with the kinetic term in Eq. (68): $[\nabla^2/(2m)] = \text{momentum}^2/\text{mass}$. The time derivative has to scale in the same way, implying that for time itself we have $[t] = \text{mass}/\text{momentum}^2$, whereas $[x] = \text{momentum}^{-1}$. Consequently, the integration measure scales like $[d^4x = dt d^3x] = \text{mass}/\text{momentum}^5$ (to compare, in the relativistic theory one would simply count $[d^4x] = \text{mass}^{-4} = \text{energy}^{-4}$).

Since the dimension of \mathcal{L} has to cancel that of the measure to give a dimensionless action, we can now infer that our field has to satisfy $[\phi] = \text{momentum}^{3/2}$, *i.e.*, even though it is a scalar field it scales with a fractional dimension (recall that in the relativistic case a scalar would have dimension energy^1). Knowing the scaling of the field and the measure, we can now proceed and deduce that of the various coupling constants.

The basic idea is very simple: each term (operator) in the Lagrangian (68) has $2n$ fields and $2m$ derivatives, giving it a total dimension of momentum^{3n+2m} . For example, the $(\phi^\dagger\phi)^2$ term with $2n = 4$ and $m = 0$ has dimension momentum^6 . Hence, to get the correct overall dimension $\text{momentum}^5/\text{mass}$ for \mathcal{L} , the coupling constant $g_2^{(0)}$ has to be $\sim 1/(\text{momentum} \times \text{mass})$. Since it is supposed to describe unresolved short-distance details, the momentum scale in the denominator should be the breakdown scale, whereas the mass scale, which as we mentioned is a feature of the nonrelativistic framework and common to all operators, is simply associated with m_ϕ . Of course, counting a single operator does not tell us much: it is the relative order of terms that matters, so we proceed to the $g_2^{(2)}$ interactions. These all come with two derivatives, which are associated with the external (small) momentum scale Q . Hence, we have $2n = 4$ and $2m = 2$, and we need to compensate the two additional powers of momentum in the numerator with two more powers of M_{hi} in the denominator, finding that the $g_2^{(2)}$ interactions are down compared to the $g_2^{(0)}$ term by a factor $(Q/M_{\text{hi}})^2$. This is exactly in line with our picture of the contact terms gradually building up the an unresolved particle exchange through a derivative expansion. For higher-body interactions, it is the larger number of fields that gives a suppression by inverse powers of M_{hi} compared to operators with fewer fields.

This kind of analysis can be much improved if something is known about which unresolved physics is supposed to be represented by which operator, and it is generally more complex if the theory involves different fields. For example, in the EFT for halo nuclei there are contact interactions associated with unresolved pion exchange, as well as those systematically accounting for the internal structure of the core field. Instead of merely putting generic powers of M_{hi} in every denominator, it can be necessary to keep track of several high scales separately to figure out the ordering of terms. Also, it is possible that the external momentum is not the only relevant low-momentum scale in the problem.

This rather abstract discussion will become clearer when we finally discuss concrete EFTs in the following sections 3 and 4. In that context, we will use the scaling of the various terms in the Lagrangian to power-count diagrams as a whole, *i.e.* to estimate the size of individual contributions composed of vertices and loops to a given physical amplitude of interest. We will then also discuss how the actual so-called scaling dimension of a field in the Lagrangian can turn out to deviate from what we estimated here based purely on dimensional grounds.

2.3.3 Fine tuning

In connection with the previous comment is another point worth stressing already here: naïve dimensional analysis resides at the beginning of EFT wisdom, not at the end, and in quite a

¹¹ This separation would be quite clear if we had not set $c = 1$, which would in fact be more appropriate for a nonrelativistic system. The reason we still do it that it allows us to still energies and momenta in the same units, *e.g.*, in MeV, following the standard convenient in nuclear physics.

few cases it turns out to be exactly what the name says: naïve. In other words, the actual scaling of a coupling constant can be quite different from what one would infer by counting dimensions, a scenario that is commonly referred to as “fine tuning.” To understand why that is consider, for example, our bosonic toy model from Sec. 2.1.1, but now assume that there already is a four- ϕ contact interaction present prior to integrating out the χ field:

$$\mathcal{L} = -\phi^\dagger (\square + m_\phi^2) \phi - \chi^\dagger (\square + m_\chi^2) \chi + g (\phi^\dagger \phi^\dagger \chi + \text{h.c.}) + h (\phi^\dagger \phi)^2. \quad (71)$$

This could, for example, come from unknown (or integrated out) short-distance physics at a yet higher scale. When we now integrate out the χ , the generated non-derivative contact term will combine with the existing one, giving a single operator in the effective low-energy Lagrangian (recall that on dimensional grounds h has to have dimensions of inverse mass squared):

$$\mathcal{L} = -\phi^\dagger (\square + m_\phi^2) \phi + \left(h - \frac{g^2}{m_\chi^2} \right) (\phi^\dagger \phi)^2 + \dots. \quad (72)$$

Now suppose we had started in the bottom-up approach and simply written down the four- ϕ contact operator with some coefficient c to be determined. According to NDA, we would assume that its scale is set by two powers of the breakdown scale in the denominator, and assuming we actually know about the more fundamental theory, we might have estimated that breakdown scale to be of the order m_χ . From Eq. (72) we see that depending on what values g and h take in the underlying theory, the actual size of c might deviate strongly from the naïve expectation, and it could even be set by a low-energy scale of the effective theory. But for this to happen, there would have to be a delicate cancellation between h and g^2/m_χ^2 , which is typically deemed unlikely given the *a priori* vast range of possible values these parameters could take; thus the term “fine tuning.” The fact that coupling constants are in fact not simple fixed numbers but get renormalized by loop effects (*i.e.*, depend on a regularization scale with a behavior determined by the renormalization group) justifies this language even more.

2.3.4 Loops and renormalization

It is indeed high time we talk about loops. Our considerations in this section so far have been limited to tree level, which is always only a first approximation in a quantum field theory. In a perturbative theory, loop contributions from virtual intermediate states are added to improve the accuracy of the result. To treat a nonperturbative system such as a bound nucleus, on the other hand, they are absolutely crucial: recall that any finite sum of diagrams in perturbation can never produce a bound state (for example, think about poles in the S-matrix, which cannot be generated through a finite sum of terms). In the field-theory language, this means that an infinite number of diagrams with increasing number of loops has to be summed to get the amplitude with the desired physical properties.

This situation is in fact familiar already from the Schrödinger equation written in the form

$$|\psi\rangle = \hat{G}_0(E) \hat{V} |\psi\rangle, \quad \hat{G}_0 = \hat{G}_0(E) = (E - \hat{H}_0)^{-1}, \quad (73)$$

which can be iterated to get $|\psi\rangle = \hat{G}_0 \hat{V} \hat{G}_0 \hat{V} |\psi\rangle = \dots$. When these operators are written out in momentum space, each propagator \hat{G}_0 corresponds to a loop. More closely related to the amplitude written down in a nonrelativistic field theory, this exercise can be repeated with the Lippmann-Schwinger equation for the T-matrix and its formal solution, the infinite Born series. Exactly this will be recovered in Sec. 3.

Of course, even in a nonperturbative theory we do not expect that *all* loop diagrams should be summed up to infinity. Generally, we want the power counting to tell us how to estimate the

contribution from a given diagram, including loop diagrams. To do that, we need to know not only what factors we pick up from vertices, but also need an estimate for the integration measure $d^4q = dq_0 d^3q$. Any loop diagram contributing to an amplitude with external momenta of the order Q will have this scale running through it a whole. It is thus natural to count the contribution from the three-momentum as $d^3q \sim Q^3$ and, recalling that in the nonrelativistic theory q_0 is a kinetic energy, $dq_0 \sim Q^2/m$. For each Schrödinger propagator we get, conversely, a factor m/Q^2 , as can be seen from Eq. (64). These simple rules combined with those for the vertices give an estimate for any diagram in the theory determined by Eq. (68).

What this discussion does not cover is the fact that loops in a quantum field theory can be—and mostly are—divergent. Compared to the loops one gets from integrating the Schrödinger or Lippmann-Schwinger equation in quantum mechanics with a potential \hat{V} , which are typically all finite, this is different in the EFT simply because our delta-function (contact) interactions are too singular to make direct sense beyond tree level. Of course, this is no different than in any other quantum field theory, and it just means that divergent loops have to be regularized (for example, by imposing a momentum cutoff or with dimensional regularization), and then suitable renormalization conditions have to be imposed to fix the various coupling constants in the effective Lagrangian. These then become functions of the renormalization scale, with a behavior governed by the renormalization group (RG). In Sec. 3 this will be discussed in detail for a bosonic EFT that describes, for example, ultracold atomic systems.

The cutoff

What the regularization of loop integrals does is most transparent with a momentum cutoff. We denote this by Λ and stress again that it has to be distinguished from the EFT breakdown scale M_{hi} . The latter determines the scale beyond which we know our EFT not to be valid. In other words, short-range dynamics corresponding to momenta larger than M_{hi} is, in general, not correctly described by the EFT. Yet from loop integrals we get contributions from states up to the UV cutoff Λ . Renormalization means to adjust the coupling constants in such a way that they compensate the wrong high-momentum loop contributions in such a way that the physics the EFT is supposed to describe comes out correctly. For momenta up to M_{hi} , we trust the EFT, so it makes sense to keep such states in loops. Hence, one should typically choose $\Lambda > M_{\text{hi}}$. Choosing it lower than the breakdown scale is possible, but this can induce corrections of the order $Q/\Lambda > Q/M_{\text{hi}}$, which is not desirable for the power counting. In the renormalized EFT, any cutoff in the interval $[M_{\text{hi}}, \infty)$ is thus an equally good choice—it does not have to be “taken to infinity.” Instead, that phrase should be understood to mean adjusting the couplings at any given finite cutoff. If this procedure is carried out numerically, it can be desirable to keep the cutoff small, but one has to make sure that in principle it *can* be varied arbitrarily.

2.4 Matching

The determination of the couplings (“low-energy constants”) in the effective Lagrangian is done by expressing a given physical quantity (e.g., a scattering amplitude or related) in terms of the couplings and then adjusting them to reproduce a known result. This can be done using experimental input or, when working top-down, by calculating the same amplitude in the more fundamental theory. Generally, this procedure is referred to as “matching.” At tree level, this is again exactly what we did by integrating out particles and found the coefficients of the generated contact interactions in terms of the original coupling and mass denominators. Once

loop diagrams are involved, the process becomes somewhat more complicated because (a) one has to make sure to use compatible regularization schemes and renormalization scales and (b) loop diagrams with lower-order vertices typically mix with higher-order tree-level diagrams. The latter is a general feature of combined loop and derivative expansions and is thus also important when matching to experimental input. While these comments may sound a bit cryptic here, they will become much clearer in the next section when we finally work with a concrete EFT.

3 Effective field theory for strongly interacting bosons

We will now use the insights from the previous sections to construct a local effective field theory for identical, spinless bosons with short-range S-wave interactions.¹² For the treatment of higher partial wave interactions the reader is referred to the literature [13–15]. The most general effective Lagrangian consistent with Galilei invariance can be written as

$$\mathcal{L} = \phi^\dagger \left(i\partial_t + \frac{\nabla^2}{2m} \right) \phi - \frac{C_0}{4} (\phi^\dagger \phi)^2 - \frac{C_2}{4} (\nabla(\phi^\dagger \phi))^2 + \frac{D_0}{36} (\phi^\dagger \phi)^3 + \dots \quad (74)$$

where m is the mass of the particles and the ellipses denote higher-derivative and/or higher-body interactions. The leading two- and three-body interactions are explicitly written out. The scaling of the coefficients C_0 , C_2 , D_0 , ... depends on the scales of the considered system. Two explicit examples, corresponding natural and unnaturally large scattering length, are discussed below.

3.1 EFT for short-range interactions

We start by considering natural system where all interactions are characterized by only one mass scale M_{hi} that we identify with the formal breakdown scale of the EFT introduced in the previous section. We will see below that this is indeed justified. Since the nonrelativistic boson fields have dimension 3/2, the coupling constants must scale as

$$C_0 \sim \frac{1}{mM_{\text{hi}}}, \quad C_2 \sim \frac{1}{mM_{\text{hi}}^3}, \quad \text{and} \quad D_0 \sim \frac{1}{mM_{\text{hi}}^4}, \quad (75)$$

such that higher dimension operators are strongly suppressed for small momenta $k \ll M_{\text{hi}}$.¹³ We first focus on the two-body system and calculate the contribution of the interaction terms in Eq. (74) to the scattering amplitude of two particles in perturbation theory. After renormalization, the result reproduces the low-energy expansion of the scattering amplitude for particles with relative momentum k and total energy $E = k^2/m$:

$$T_2(E) = \frac{8\pi}{m} \frac{1}{k \cot \delta_0(k) - ik} = -\frac{8\pi a}{m} (1 - iak + (a r_e/2 - a^2)k^2 + \mathcal{O}(k^3)), \quad (76)$$

¹² See Ref. [12] for a similar discussion with a focus on applications in ultracold atoms.

¹³ Note that coupling constants scale with the particle mass as $1/m$ in nonrelativistic theories. This can be seen by rescaling all energies as $q_0 \rightarrow \tilde{q}_0/m$ and all time coordinates as $t \rightarrow \tilde{t}m$, so that dimensionful quantities are measured in units of momentum. Demanding that the action is independent of m , it follows that the coupling constants must scale as $1/m$.

where the effective range expansion for short-range interactions $k \cot \delta_0(k) = -1/a + r_e k^2/2 + \mathcal{O}(k^4)$ has been used.

Since all coefficients of the effective Lagrangian are natural (scaling with inverse powers of M_{hi}), it is sufficient to count the powers of small momenta Q in scattering amplitudes to determine the scaling of the amplitudes with M_{lo} . The correct dimensions are made up with appropriate factors of M_{hi} contained in the coupling constants (*cf.* Eq. (75)). For a general two-body amplitude with L loops and V_{2i} interaction vertices with $2i$ derivatives, we thus have $T_2 \sim Q^v$ where the power v is given by

$$v = 3L + 2 + \sum_i (2i - 2)V_{2i} \geq 0. \quad (77)$$

Here we have used that loop integrations contribute a factor k^5 and propagators a factor k^{-2} in nonrelativistic theories. The values of the coupling constants C_0 and C_2 can be determined by matching to Eq. (76). In the lowest two orders only C_0 contributes.

3. Exercise: Derive Eq. (77) using the topological identity for Feynman diagrams:

$$L = I - V + 1, \quad (78)$$

with L , V , and I the total number of loops, vertices, and internal lines respectively.

The contact interactions in Eq. (74) are ill-defined unless an ultraviolet cutoff is imposed on the momenta in loop diagrams. This can be seen by writing down the off-shell amplitude for two-body scattering at energy E in the center-of-mass frame at second order in perturbation theory:

$$T_2(E) \approx -C_0 - \frac{i}{2} C_0^2 \int \frac{d^3 q}{(2\pi)^3} \int \frac{dq_0}{2\pi} \frac{1}{q_0 - q^2/2m + i\epsilon} \frac{1}{E - q_0 - q^2/2m + i\epsilon} + \dots$$

The two terms correspond to the first two diagrams in Fig. 4. The intermediate lines have

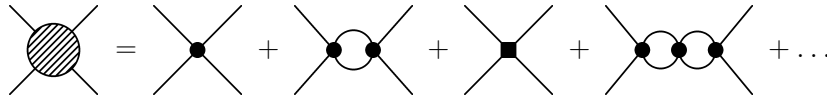


Fig. 4 Diagrammatic expression for the two-body scattering amplitude T_2 . The circle (square) denotes a C_0 (C_2) interaction, respectively.

momenta $\pm \mathbf{q}$. The integral over q_0 in Eq. (79) is easily evaluated using contour integration:

$$T_2(E) \approx -C_0 - \frac{1}{2} C_0^2 \int \frac{d^3 q}{(2\pi)^3} \frac{1}{E - q^2/m + i\epsilon} + \dots \quad (79)$$

The integral over \mathbf{q} diverges. It can be regularized by imposing an ultraviolet cutoff $|\mathbf{q}| < \Lambda$. Taking the limit $\Lambda \gg |E|^{1/2}$, the amplitude reduces to¹⁴

$$T_2(E) \approx -C_0 + \frac{m C_0^2}{4\pi^2} \left(\Lambda - \frac{\pi}{2} \sqrt{-mE - i\epsilon} \right) + \dots \quad (80)$$

¹⁴ If the calculation was carried out in a frame in which the total momentum of the two scattering particles was nonzero, the simple cutoff $|\mathbf{q}| < \Lambda$ would give a result that does not respect Galilean invariance. To obtain a Galilean-invariant result requires either using a more sophisticated cutoff or else imposing the cutoff $|\mathbf{q}| < \Lambda$ only after an appropriate shift in the integration variable \mathbf{q} .

The dependence on the ultraviolet cutoff Λ can be consistently eliminated by a perturbative renormalization procedure. A simple choice is to eliminate the parameter C_0 in favor of the scattering length a , which is given by Eq. (76):

$$a \approx \frac{mC_0}{8\pi} \left(1 - \frac{mC_0\Lambda}{4\pi^2} + \dots \right). \quad (81)$$

Inverting this expression to obtain C_0 as a function of a we obtain

$$C_0 \approx \frac{8\pi a}{m} \left(1 + \frac{2a\Lambda}{\pi} + \dots \right), \quad (82)$$

where we have truncated at second order in a . Inserting the expression for C_0 into Eq. (80) and expanding to second order in a , we obtain the renormalized expression for the amplitude:

$$T_2(E) \approx -\frac{8\pi a}{m} \left(1 + a\sqrt{-mE - i\varepsilon} + \dots \right) = -\frac{8\pi a}{m} (1 - iak + \dots). \quad (83)$$

If we evaluate this at the on-shell point $E = k^2/m$ and insert it into Eq. (80), we find that it reproduces the first two terms in the expansion of the universal scattering amplitude in Eq. (76) in powers of ka . By calculating $T_2(E)$ to higher order in perturbation theory, we can reproduce the low-momentum expansion of Eq. (76) to higher order in ka . At the next order, the C_2 term will contribute at tree level while C_0 will contribute at the two-loop level. Thus a perturbative treatment of the EFT reproduces the low-momentum expansion of the two-body scattering amplitude. The perturbative approximation is valid only if the momentum satisfies $k \ll 1/a$.

A more interesting case occurs when the scattering length is large, but all other effective range coefficients are still determined by the scale M_{hi} : $k \sim 1/|a| \sim M_{\text{lo}} \ll M_{\text{hi}} \sim 1/r_e$. This scenario is able to support shallow bound states with binding momentum of order $1/a$ and is relevant to ultracold atoms close to a Feshbach resonance and very low-energy nucleons. The scaling of the operators is then modified to:

$$C_0 \sim \frac{1}{mM_{\text{lo}}}, \quad C_2 \sim \frac{1}{mM_{\text{lo}}^2 M_{\text{hi}}}, \quad \text{and} \quad D_0 \sim \frac{1}{mM_{\text{lo}}^4}. \quad (84)$$

The factors of M_{lo} in amplitudes can now come from small momenta and from the coupling constants. Above we adjusted the scaling of the three-body coupling D_0 as well, foreclosing a result discussed below Eq. (98).

With the scaling as in Eq. (84), the power counting expression in Eq. (77) is therefore modified to

$$\nu = 3L + 2 + \sum_i (i-3)V_{2i} \geq -1. \quad (85)$$

If we are interested in two-body observables involving energy $E \sim 1/a^2$, such as shallow bound or virtual states, we must resum the diagrams involving only C_0 interactions to all orders [16, 17]. Without this resummation, our EFT would break down not at M_{hi} , but already at the much smaller scale $1/|a| \sim M_{\text{lo}}$. In the scenario assumed here, all higher-derivative two-body interactions (C_2 and beyond) still involve inverse powers of M_{hi} and are thus perturbative.

The resummation of C_0 interactions is most easily accomplished by realizing that the corresponding Feynman diagrams in Fig. 4 form a geometric series. Summing the geometric series, the exact expression for the amplitude is

$$T_2(E) = -C_0 \left[1 + \frac{mC_0}{4\pi^2} \left(\Lambda - \frac{\pi}{2} \sqrt{-mE - i\varepsilon} \right) \right]^{-1}. \quad (86)$$

Alternatively, we can use the fact that summing the C_0 diagrams in Fig. 4 is equivalent to solving the following integral equation:

$$T_2(E) = -C_0 - \frac{i}{2} C_0 \int \frac{d^3 q}{(2\pi)^3} \int \frac{dq_0}{2\pi} \frac{1}{q_0 - q^2/2m + i\epsilon} \frac{1}{E - q_0 - q^2/2m + i\epsilon} T_2(E). \quad (87)$$

The integral equation is expressed diagrammatically in Fig. 5. Since the function $T_2(E)$ is

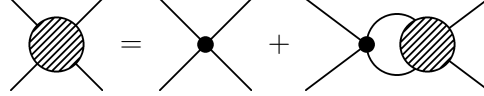


Fig. 5 Integral equation for the two-body scattering amplitude T_2 at leading order in the case of large scattering length. Notation as in Fig. 4.

independent of \mathbf{q} and q_0 , it can be pulled outside of the integral in Eq. (87). The integral can be regularized by imposing an ultraviolet cutoff Λ . The integral equation is now trivial to solve and the solution is given in Eq. (86).

The expression for the resummed two-body amplitude in Eq. (86) depends on the parameter C_0 in the Lagrangian and on the ultraviolet cutoff Λ . As in the perturbative case, renormalization can be implemented by eliminating C_0 in favor of a low-energy observable, such as the scattering length a . Matching the resummed expression to the effective range expansion for T_2 , we obtain

$$C_0 = \frac{8\pi a}{m} \left(1 - \frac{2a\Lambda}{\pi} \right)^{-1}. \quad (88)$$

Given a fixed ultraviolet cutoff Λ , this equation prescribes how the parameter C_0 must be tuned in order to give the scattering length a . Note that for $\Lambda \gg 1/|a|$, the coupling constant C_0 is always negative regardless of the sign of a . Eliminating C_0 in Eq. (86) in favor of a , we find that the resummed amplitude reduces to

$$T_2(E) = \frac{8\pi}{m} \frac{1}{-1/a + \sqrt{-mE - i\epsilon}}, \quad (89)$$

which reproduces the effective range expansion of the scattering amplitude by construction. In this simple case, we find that our renormalization prescription eliminates the dependence on Λ completely. In general, we should expect it to only be suppressed by powers of $1/(a\Lambda)$ or mE/Λ^2 . A final step of taking the limit $\Lambda \rightarrow \infty$ would then be required to obtain results that are completely independent of Λ . The first correction to Eq. (89) is given by the C_2 interaction. The corresponding diagrams are shown in Fig. 6. After the matching, the final result for the

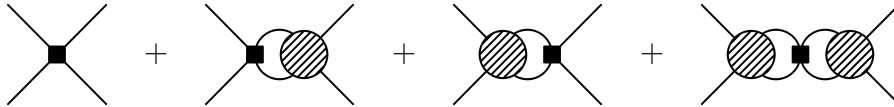


Fig. 6 Next-to-leading order correction to T_2 . Notation as in Fig. 4.

scattering amplitude at next-to-leading order is

$$T_2(E) = \frac{8\pi}{m} \left(\frac{1}{-1/a + \sqrt{-mE - i\epsilon}} + \frac{r_e m E / 2}{(-1/a + \sqrt{-mE - i\epsilon})^2} \right), \quad (90)$$

where r_e is the effective range. The derivation of this expression will be left as an exercise.

4. Exercise: Derive the next-to-leading order correction in Eq. (90) by calculating the loop diagrams in Fig. 6. Neglect all terms that vanish as $\Lambda \rightarrow \infty$. Introduce a next-to-leading order piece of C_0 to cancel the cubic divergence.

3.2 Dimer field formalism

In applications to systems with more than two particles, it is often useful to rewrite the EFT for short-range interactions specified by the Lagrangian (74) using so-called dimer fields d [18]:

$$\begin{aligned} \mathcal{L} = & \phi^\dagger \left(i\partial_t + \frac{\nabla^2}{2m} \right) \phi + g_0 d^\dagger d + g_2 d^\dagger \left(i\partial_t + \frac{\nabla^2}{4m} \right) d + \dots \\ & - y \left(d^\dagger \phi^2 + \phi^{\dagger 2} d \right) - d_0 d^\dagger d \phi^\dagger \phi + \dots \end{aligned} \quad (91)$$

One important feature of this Lagrangian is that there is no direct two-body contact interaction term $(\phi^\dagger \phi)^2$. All interactions between ϕ particles are mediated via exchange of a dimer field d , *i.e.*, we have effectively performed a Hubbard–Stratonovich transformation. Eliminating the dimer field d by using its equations of motion, it can be shown that the physics of this EFT is equivalent to the Lagrangian (74).

Note that the Lagrangian (91) contains one more free parameter than the Lagrangian (74). Thus some parameters are redundant. For the leading-order case ($g_n = 0$ for $n \geq 2$), *e.g.*, we find explicitly,

$$C_0 = \frac{4y^2}{g_0}, \quad (92)$$

such that y and g_0 are not independent. Higher-order corrections can be obtained by including a kinetic-energy term for the dimer field. The constants g_0 and y then become independent and can be related to combinations of C_0 and C_2 in the theory without dimers. Here, we only discuss the leading-order case.

5. Exercise: Derive Eq. (92) using the classical equation of motion for d .

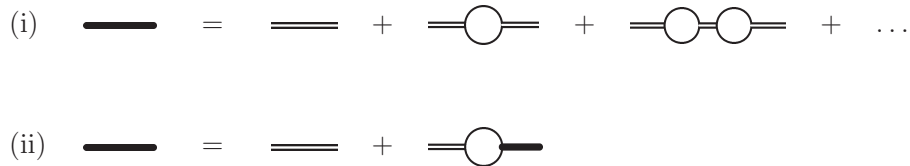


Fig. 7 Diagrammatic equations for the full dimer propagator $iD(P_0, P)$. Thin (thick) solid lines represent particle (full dimer) propagators. Double lines indicate bare dimer propagators. (i) perturbative expansion in powers of y , (ii) integral equation summing the geometric series in (i).

The bare propagator for the dimer field is simply the constant i/g_0 , which corresponds to no propagation in space or time. However, there are corrections to the dimer propagator

from the diagrams in Fig. 7(i) which allow the dimer to propagate. This is completely analogous to the geometric series we found we had to sum to obtain the leading-order scattering amplitude. In Feynman diagrams, we represent the full dimer propagator $iD(P_0, P)$ by a thick solid line. We can calculate the full dimer propagator by solving the simple integral equation shown in Fig. 7(ii). The loop on the right side is just the integral in Eq. (79), with E replaced by $P_0 - P^2/(4m)$, where P_0 and \mathbf{P} are the energy and momentum of the dimer. The solution for the full dimer propagator is

$$iD(P_0, P) = \frac{2\pi i}{y^2 m} \left[\frac{2\pi g_0}{y^2 m} + \frac{2}{\pi} \Lambda - \sqrt{-mP_0 + P^2/4 - i\epsilon} \right]^{-1}, \quad (93)$$

where as before Λ is a cutoff on the loop momentum in the bubbles. Using Eq. (92) and making the substitution given in Eq. (88), the expression for the complete dimer propagator is

$$iD(P_0, P) = -\frac{2\pi i}{y^2 m} \left[-1/a + \sqrt{-mP_0 + P^2/4 - i\epsilon} \right]^{-1}. \quad (94)$$

Note that all the dependence on the ultraviolet cutoff is now in the multiplicative factor $1/y^2$. The complete dimer propagator differs from the off-shell two-body amplitude T_2 in Eq. (89) only by a multiplicative constant. For $a > 0$, it has a pole at $P_0 = -1/(ma^2) + P^2/4$ corresponding to a dimer of momentum \mathbf{P} and binding energy $B_2 = 1/(ma^2)$. As P_0 approaches the dimer pole, the limiting behavior of the propagator is

$$D(P_0, P) \longrightarrow \frac{Z_D}{P_0 - (-1/(ma^2) + P^2/4) + i\epsilon}, \quad (95)$$

where the residue factor is

$$Z_D = \frac{4\pi}{am^2 y^2}. \quad (96)$$

If we regard the composite operator d as a quantum field that annihilates and creates dimers, then Z_D is the wave function renormalization constant for that field. The renormalized propagator $Z_D^{-1}D(P_0, P)$ is completely independent of the ultraviolet cutoff.

3.3 Three-body system

We now study the amplitude for particle-dimer scattering T_3 . The simplest diagram we can write down involving only two-body interactions is the exchange of a particle between in- and outgoing dimers. With the scaling of low-energy constants as in Eq. (84), the power counting implies that all diagrams that are chains of such exchanges are equally important, *i.e.*, they have to be summed up nonperturbatively. Just like in the two-body case, this can be written as an integral equation. Also including the three-body interaction (note $D_0 \rightarrow d_0$ in the Lagrangian with dimer fields), we get the result that is shown diagrammatically in Fig. 8.¹⁵

Omitting the three-body interaction, this is exactly the well-known Skorniakov-Ter-Martirosian (STM) integral equation [19], which the EFT with Lagrangian (91) reproduces by construction. In addition, EFT provides a clear method to renormalize this equation with a three-body interaction and thus remove its pathologies (discussed below).

In Fig. 8, all external lines are understood to be amputated. It simply gives the non-perturbative solution of the three-body problem for the interaction terms proportional to g_0 , y , and d_0 in Eq. (91).

¹⁵ Note that this amplitude is well defined even if $a < 0$ and there is no two-body bound state. In this case particle lines must be attached to the external dimer propagators to obtain the 3-particle scattering amplitude.

The two tree diagrams on the right side of Fig. 8 constitute the inhomogeneous term in the integral equation. An iterative ansatz for the solution of this equation shows that all diagrams with the g_0 , y , and d_0 interactions are generated by the iteration. Note also that the thick black lines in Fig. 8 represent the full dimer propagator given in Eq. (94).

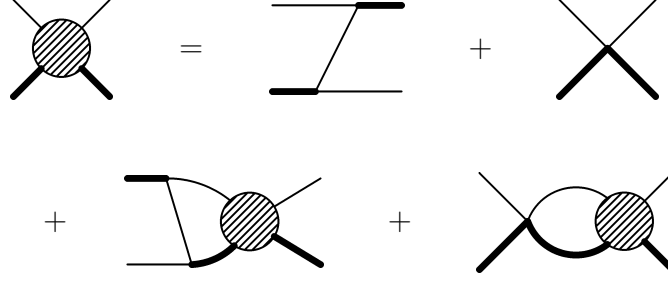


Fig. 8 The integral equation for the three-body amplitude T_3 . Thin (thick) solid lines represent particle (full dimer) propagators. External lines are amputated.

In the center-of-mass frame, we can take the external momenta of the particle and dimer to be $-\mathbf{p}$ and $+\mathbf{p}$ for the incoming lines and $-\mathbf{k}$ and $+\mathbf{k}$ for the outgoing lines. We take their energies to be E_A and $E - E_A$ for the incoming lines and E'_A and $E - E'_A$ for the outgoing lines. The amplitude T_3 is then a function of the momenta \mathbf{p} and \mathbf{k} and the energies E , E_A and E'_A . The integral equation involves a loop over the momentum $-\mathbf{q}$ and energy q_0 of a virtual particle. Using the Feynman rules encoded in the Lagrangian (91), we obtain

$$T_3(\mathbf{p}, \mathbf{k}; E, E_A, E'_A) = - \left[\frac{4y^2}{E - E_A - E'_A - (\mathbf{p} + \mathbf{k})^2/(2m) + i\epsilon} + d_0 \right] + \frac{2\pi i}{my^2} \int \frac{dq_0}{2\pi} \int \frac{d^3q}{(2\pi)^3} \left[\frac{4y^2}{E - E_A - q_0 - (\mathbf{p} + \mathbf{q})^2/(2m) + i\epsilon} + d_0 \right] \times \frac{1}{q_0 - q^2/(2m) + i\epsilon} \frac{T_3(\mathbf{q}, \mathbf{k}; E, q_0, E'_A)}{1/a - \sqrt{-m(E - q_0) + q^2/4} - i\epsilon}. \quad (97)$$

The integral over q_0 can be evaluated by contour integration. This sets $q_0 = q^2/(2m)$, so the amplitude T_3 inside the integral has the incoming particle on-shell.

We obtain a simpler integral equation if we also set the energies of both the initial and final particles in T_3 on-shell: $E_A = p^2/(2m)$, $E'_A = k^2/(2m)$. Thus only the dimer lines have energies that are off-shell. The resulting integral equation is

$$T_3\left(\mathbf{p}, \mathbf{k}; E, \frac{p^2}{2m}, \frac{k^2}{2m}\right) = -4my^2 \left[\frac{1}{mE - (p^2 + \mathbf{p} \cdot \mathbf{k} + k^2) + i\epsilon} + \frac{d_0}{4my^2} \right] - 8\pi \int \frac{d^3q}{(2\pi)^3} \left[\frac{1}{mE - (p^2 + \mathbf{p} \cdot \mathbf{q} + q^2) + i\epsilon} + \frac{d_0}{4my^2} \right] \times \frac{T_3(\mathbf{q}, \mathbf{k}; E, q^2/(2m), k^2/(2m))}{-1/a + \sqrt{-mE + 3q^2/4} - i\epsilon}. \quad (98)$$

This is an integral equation with three integration variables for an amplitude T_3 that depends explicitly on seven independent variables. There is also an additional implicit variable provided by an ultraviolet cutoff $|\mathbf{q}| < \Lambda$ on the loop momentum.

If we set $d_0 = 0$ and ignore the ultraviolet cutoff, the integral equation in Eq. (98) is equivalent to the Skorniakov-Ter-Martirosian (STM) equation, an integral equation for three particles interacting via zero-range two-body forces derived by Skorniakov and Ter-Martirosian in 1957 [19]. It was shown by Danilov that the STM equation has no unique solution in the case of identical bosons [20]. He also pointed out that a unique solution could be obtained if one three-body binding energy is fixed. Kharchenko was the first to solve the STM equation with a finite ultraviolet cutoff that was tuned to fit observed three-body data. Thus the cutoff was treated as an additional parameter [21]. When we discuss the running of d_0 , we will see that this *ad hoc* procedure is indeed justified and emerges naturally when the three-body equation is renormalized [22].

Here we restrict our attention to the sector of the three-body problem with total orbital angular momentum $L = 0$ where the three-body interaction contributes. For higher L , the original STM equation has a unique solution and can be solved numerically without complication.

The projection onto $L = 0$ can be accomplished by averaging the integral equation over the cosine of the angle between \mathbf{p} and \mathbf{k} : $x = \mathbf{p} \cdot \mathbf{k} / (pk)$. It is also convenient to multiply the amplitude T_3 by the wave function renormalization factor Z_D given in Eq. (96). We will denote the resulting amplitude by T_3^0 :

$$T_3^0(p, k; E) \equiv Z_D \int_{-1}^1 \frac{dx}{2} T_3(\mathbf{p}, \mathbf{k}; E, p^2/(2m), k^2/(2m)). \quad (99)$$

Furthermore, it is convenient to express the three-body coupling constant in the form

$$d_0 = -\frac{4my^2}{\Lambda^2} H(\Lambda). \quad (100)$$

Since H is dimensionless, it can only be a function of the dimensionless variables $a\Lambda$ and Λ/Λ_* , where Λ_* is a three-body parameter defined below. We will find that H is a function of Λ/Λ_* only.

The resulting integral equation is:

$$\begin{aligned} T_3^0(p, k; E) = & \frac{16\pi}{ma} \left[\frac{1}{2pk} \ln \left(\frac{p^2 + pk + k^2 - mE - i\epsilon}{p^2 - pk + k^2 - mE - i\epsilon} \right) + \frac{H(\Lambda)}{\Lambda^2} \right] \\ & + \frac{4}{\pi} \int_0^\Lambda dq q^2 \left[\frac{1}{2pq} \ln \left(\frac{p^2 + pq + q^2 - mE - i\epsilon}{p^2 - pq + q^2 - mE - i\epsilon} \right) + \frac{H(\Lambda)}{\Lambda^2} \right] \\ & \times \frac{T_3^0(q, k; E)}{-1/a + \sqrt{3q^2/4 - mE - i\epsilon}}. \quad (101) \end{aligned}$$

Note that the ultraviolet cutoff Λ on the integral over q has been made explicit. A change in the endpoint Λ of the loop integral should be compensated by the Λ -dependence of the function H in Eq. (101). More specifically, H must be tuned as a function of Λ so that the cutoff dependence of the solution $T_3^0(p, k; E)$ of Eq. (101) decreases as a power of Λ . This will guarantee that $T_3^0(p, k; E)$ has a well-behaved limit as $\Lambda \rightarrow \infty$. The renormalization group behavior of H will be discussed in detail below. In the next subsection, we show how different three-body observables can be obtained from the solution $T_3^0(p, k; E)$ of Eq. (101).

6. Fill in the gaps in the above derivation of Eq. (101) and generalize the derivation to general angular momentum L .

3.4 Three-body observables

The solution $T_3^0(p, k; E)$ to the three-body integral equation (101) encodes all information about three-body observables in the sector with total orbital angular momentum quantum number $L = 0$. In particular, it contains information about the binding energies $B_3^{(n)}$ of the three-body bound states [23]. For a given ultraviolet cutoff Λ , the amplitude $T_3^0(p, k; E)$ has a finite number of poles in E corresponding to the bound states whose binding energies are less than about Λ^2 . As Λ increases, new poles emerge corresponding to deeper bound states. In the limit $\Lambda \rightarrow \infty$, the locations of these poles approach the energies $-B_3^{(n)}$ of the three-body bound states. The residues of the poles of $T_3^0(p, k; E)$ factor into functions of p and functions of k :

$$T_3^0(p, k; E) \longrightarrow \frac{\mathcal{B}^{(n)}(p)\mathcal{B}^{(n)}(k)}{E + B_3^{(n)}}, \quad \text{as } E \rightarrow -B_3^{(n)}. \quad (102)$$

Matching the residues of the poles on both sides of Eq. (101), we obtain the bound-state equation

$$\begin{aligned} \mathcal{B}^{(n)}(p) = & \frac{4}{\pi} \int_0^\Lambda dq q^2 \left[\frac{1}{2pq} \ln \frac{p^2 + pq + q^2 - mE - i\epsilon}{p^2 - pq + q^2 - mE - i\epsilon} + \frac{H(\Lambda)}{\Lambda^2} \right] \\ & \times \left[-1/a + \sqrt{3q^2/4 - mE - i\epsilon} \right]^{-1} \mathcal{B}^{(n)}(q). \end{aligned} \quad (103)$$

The values of E for which this homogeneous integral equation has solutions are the energies $-B_3^{(n)}$ of the three-body states. For a finite ultraviolet cutoff Λ , the spectrum of $B_3^{(n)}$ is cut off around Λ^2 .

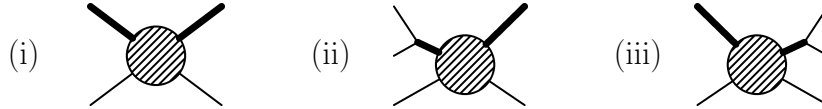


Fig. 9 Amplitudes for (i) particle-dimer scattering, (ii) three-body recombination, and (iii) three-body breakup. Diagrams (ii) [(iii)] should be summed over the three pairs of particles that can interact first [last]. Notation as in Fig. 8.

The S-wave phase shifts for particle-dimer scattering can be determined from the solution $T_3^0(p, k; E)$ to the integral equation (101). The T-matrix element for the elastic scattering of an particle and a dimer with momenta k is given by the amplitude T_3^0 evaluated at the on-shell point $p = k$ and $E = -B_2 + 3k^2/(4m)$ and multiplied by a wave function renormalization factor $Z_D^{1/2}$ for each dimer in the initial or final state. It can be represented by the Feynman diagram in Fig. 9(i). The blob represents the amplitude T_3 or equivalently $Z_D^{-1}T_3^0$. The external double lines are amputated and correspond to asymptotic dimers and are associated with factors $Z_D^{1/2}$.

The S-wave contribution to the T-matrix element is

$$T_{PD \rightarrow PD}^0 = T_3^0(k, k; 3k^2/(4m) - 1/(ma^2)), \quad (104)$$

where $B_2 = 1/(ma^2)$ has been used. Note that the factors of Z_D multiplying T_3^0 cancel. The differential cross section for elastic particle-dimer scattering is

$$d\sigma_{PD \rightarrow PD} = \frac{2m}{3k} |T_{PD \rightarrow PD}(k)|^2 \frac{km}{6\pi^2} d\Omega. \quad (105)$$

The flux factor $2m/(3k)$ is the inverse of the relative velocity of the particle and the dimer. The phase space factor $km d\Omega/(6\pi^2)$ takes into account energy and momentum conservation and the standard normalization of momentum eigenstates:

$$\int \frac{d^3 p_A}{(2\pi)^3} \frac{d^3 p_D}{(2\pi)^3} (2\pi)^4 \delta^3(\mathbf{p}_A + \mathbf{p}_D) \delta(p_A^2/(2m) + p_D^2/(4m) - E) = \frac{m}{6\pi^2} (4mE/3)^{1/2} \int d\Omega. \quad (106)$$

The S-wave phase shift for particle-dimer scattering is related to the T-matrix element via

$$\frac{1}{k \cot \delta_0^{PD}(k) - ik} = \frac{m}{3\pi} T_3^0(k, k; 3k^2/(4m) - 1/(ma^2)). \quad (107)$$

In particular, the particle-dimer scattering length is given by

$$a_{PD} = -\frac{m}{3\pi} T_3^0(0, 0; -1/(ma^2)). \quad (108)$$

The threshold rate for three-body recombination can also be obtained from the solution $T_3^0(p, k; E)$ to the three-body integral equation in Eq. (101). This is possible only at threshold, because a 3-particle scattering state becomes pure $L = 0$ only in the limit that the energies of the particles go to zero. The T-matrix element for the recombination process can be represented by the Feynman diagram in Fig. 9(ii) summed over the three pairs of particle lines that can attach to the dimer line. The blob represents the amplitude $Z_D^{-1} T_3^0$ evaluated at the on-shell point $p = 0$, $k = 2/(\sqrt{3}a)$, and $E = 0$. The solid line represents the dimer propagator $iD(0, 0)$ evaluated at zero energy and momentum $2/(\sqrt{3}a)$, which is given by Eq. (93). The factor for the particle-dimer vertex is $-i2\gamma$. The wave function renormalization factor $Z_D^{1/2}$ for the final-state dimer is given by Eq. (96). In the product of factors multiplying T_3^0 , the dependence on γ and Λ can be eliminated in favor of the scattering length a . Taking into account a factor of 3 from the three Feynman diagrams, the T-matrix element is

$$T_{PD \rightarrow PPP} = 6\sqrt{\pi a^3} T_3^0(0, 2/(\sqrt{3}a); 0). \quad (109)$$

The differential rate dR for the recombination of three particles with energies small compared to the dimer binding energy can be expressed as

$$dR = |T_{PPP \rightarrow PD}|^2 \frac{km}{6\pi^2} d\Omega, \quad (110)$$

where $k = 2/(\sqrt{3}a)$. The threshold rate for three-body breakup can be obtained in a similar way from the Feynman diagram in Fig. 9(iii)

The inhomogeneous integral equation for the off-shell particle dimer amplitude, Eq. (101), and the homogeneous equation, Eq. (103), for the three-body binding energies afford no analytical solution. They are usually solved by discretizing the integrals involved and solving the resulting matrix problems numerically.

3.5 Renormalization group limit cycle

The form of the full renormalized dimer propagator in Eq. (94) is consistent with the continuous scaling symmetry

$$a \longrightarrow \lambda a, \quad E \longrightarrow \lambda^{-2} E, \quad (111)$$

for any positive real number λ . In the integral equation (101), this scaling symmetry is broken by the ultraviolet cutoff on the integral and by the three-body terms proportional to H/Λ^2 . To see that the cutoff and the three-body terms are essential, we set $H = 0$ and take $\Lambda \rightarrow \infty$. The resulting integral equation has exact scaling symmetry. We should therefore expect its solution $T_3^0(p, k; E)$ to behave asymptotically as $p \rightarrow \infty$ like a pure power of p . Neglecting the inhomogeneous term, neglecting E and $1/a^2$ compared to q^2 , and setting $T_3^0 \approx p^{s-1}$, the integral equation reduces to [20]

$$p^{s-1} = \frac{4}{\sqrt{3}\pi p} \int_0^\infty dq q^{s-1} \ln \frac{p^2 + pq + q^2}{p^2 - pq + q^2}. \quad (112)$$

Making the change of variables $q = xp$, the dependence on p drops out, and we obtain

$$1 = \frac{4}{\sqrt{3}\pi} \int_0^\infty dx x^{s-1} \ln \frac{1+x+x^2}{1-x+x^2}. \quad (113)$$

The integral is a Mellin transform that can be evaluated analytically. The resulting equation for s is

$$1 = \frac{8}{\sqrt{3}s} \frac{\sin(\pi s/6)}{\cos(\pi s/2)}. \quad (114)$$

The solutions with the lowest values of $|s|$ are purely imaginary: $s = \pm i s_0$, where $s_0 \approx 1.00624$. The most general asymptotic solution therefore has two arbitrary constants:

$$T_3^0(p, k; E) \longrightarrow A_+ p^{-1+i s_0} + A_- p^{-1-i s_0}, \quad \text{as } p \rightarrow \infty. \quad (115)$$

The inhomogeneous term in the integral equation (101) will determine one of the constants. The role of the three-body term in the integral equation is to determine the other constant, thus giving the integral equation a unique solution.

By demanding that the solution of the integral equation (101) has a well-defined limit as $\Lambda \rightarrow \infty$, Bedaque *et al.* deduced the Λ -dependence of H and therefore of d_0 [22]. The leading dependence on Λ on the right side of the three-body integral equation in Eq. (101) as $\Lambda \rightarrow \infty$ is a log-periodic term of order Λ^0 that comes from the region $q \sim \Lambda$. There are also contributions of order $1/\Lambda$ from the region $|a|^{-1}, k, |E|^{1/2} \ll q \ll \Lambda$, which have the form

$$\frac{8}{\pi\sqrt{3}} \int^\Lambda dq \left(\frac{1}{q^2} + \frac{H(\Lambda)}{\Lambda^2} \right) (A_+ q^{+i s_0} + A_- q^{-i s_0}). \quad (116)$$

The sum of the two terms will decrease even faster as $1/\Lambda^2$ if we choose the function H to have the form

$$H(\Lambda) = \frac{A_+ \Lambda^{i s_0} / (1 - i s_0) + A_- \Lambda^{-i s_0} / (1 + i s_0)}{A_+ \Lambda^{i s_0} / (1 + i s_0) + A_- \Lambda^{-i s_0} / (1 - i s_0)}. \quad (117)$$

The tuning of H that makes the term in Eq. (116) decrease like $1/\Lambda^2$ also suppresses the contribution from the region $q \sim \Lambda$ by a power of $1/\Lambda$ so that it goes to 0 in the limit $\Lambda \rightarrow \infty$. By choosing $A_\pm = (1 + s_0^2)^{1/2} \Lambda_*^{\mp i s_0} / 2$ in Eq. (117), we obtain [22]

$$H(\Lambda) \approx \frac{\cos[s_0 \ln(\Lambda/\Lambda_*) + \arctan s_0]}{\cos[s_0 \ln(\Lambda/\Lambda_*) - \arctan s_0]}. \quad (118)$$

This equation defines a three-body scaling-violation parameter Λ_* with dimensions of momentum. The value of Λ_* can be fixed from a three-body datum. All other three-body observables can then be predicted. If Eq. (118) is substituted back into the three-body equation (101) for numerical calculations, it must be multiplied by a normalization factor $b \approx 1$ whose precise value depends on the details of the regularization [24].

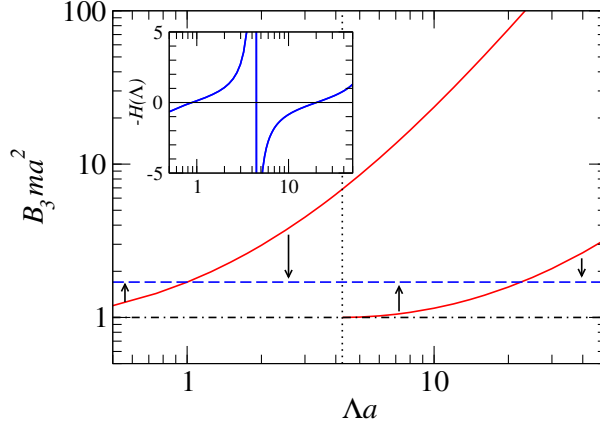


Fig. 10 Unrenormalized three-body energies B_3 as a function of the momentum cutoff Λ (solid lines). The dotted line indicates the cutoff where a new three-body state appears at the particle-dimer threshold (dash-dotted line). The dashed line shows a hypothetical renormalized energy. The inset shows the running of the three-body force $d_0(\Lambda) \sim -H(\Lambda)$ with Λ .

Note that H is a π -periodic function of $s_0 \ln(\Lambda/\Lambda_*)$, so Λ_* is defined only up to a multiplicative factor of $(e^{\pi/s_0})^n$, where n is an integer. Thus the scaling symmetry of Eq. (111) is broken to the discrete subgroup of scaling transformations with multiples of the preferred scaling factor $\lambda = e^{\pi/s_0}$. This discrete scaling symmetry is, e.g., evident in the geometric spectrum of three-body Efimov states [23] in the unitary limit ($1/a = 0$) that naturally emerge in this EFT:

$$B_3^{(n)} \approx 0.15 \lambda^{2(n-n_*)} \frac{\Lambda_*^2}{m}, \quad (119)$$

where n_* an integer labeling the state with binding energy $0.15 \Lambda_*^2/m$.¹⁶ The discrete scaling symmetry becomes also manifest in the log-periodic dependence of three-body observables on the scattering length. This log-periodic behavior is the hallmark signature of a renormalization group limit cycle. It has been observed experimentally in the three-body recombination spectra of ultracold atomic gases close to a Feshbach resonance [25, 26].

The physics of the renormalization procedure is illustrated in Fig. 10 where we show the unrenormalized three-body binding energies B_3 in the case of positive scattering length as a function of the cutoff Λ (solid line). As the cutoff Λ is increased, B_3 increases asymptotically as Λ^2 . At a certain cutoff (indicated by the dotted line), a new bound state appears at the boson-dimer threshold. This pattern repeats every time the cutoff increases by the discrete scaling factor $\exp(\pi/s_0)$. Now assume that we adopt the renormalization condition that the shallowest state should have a constant energy given by the dashed line. At small values of the cutoff, we need an attractive three-body force to increase the binding energy of the shallowest state as indicated by the arrow. As the cutoff is increased further, the required attractive contribution becomes smaller and around $\Lambda a = 1.1$ a repulsive three-body force is required (downward arrow). Around $\Lambda a = 4.25$, a new three-body state appears at threshold and we cannot satisfy the renormalization condition by keeping the first state at the required energy anymore. The number of bound states has changed and there is a new shallow state in the system. At this point the three-body force turns from repulsive to attractive to move the new state to the required energy. The corresponding running of the three-body force with the cutoff Λ is shown in the inset. After renormalization, the first state is still present as a

¹⁶ For a detailed discussion of the Efimov effect for finite scattering length and applications to ultracold atoms, see Ref. [12].

deep state with large binding energy, but for threshold physics its presence can be ignored. This pattern goes on further and further as the cutoff is increased [27].

4 Effective field theory for nuclear few-body systems

4.1 Overview

Depending on the physics one wishes to describe, there are several effective field theories for low-energy nuclear physics to choose from. They differ in the set of effective degrees of freedom, their expansion point (typical low-energy scale) and range of applicability. Chiral effective field theory includes nucleons and pions and is designed as an expansion about the so-called “chiral limit,” *i.e.*, the scenario where the quark masses are exactly zero such that the pions emerge as exactly massless Goldstone bosons from the spontaneous breaking of chiral symmetry. In reality, the quark-masses are nonzero such that the pions become “pseudo-Goldstone” bosons with a small (compared to typical QCD scales like m_ρ or M_N) mass m_π . Chiral EFT takes this as a typical low scale so that its power counting is designed for momenta of the order $Q \sim m_\pi$; we come back to this in Sec. 5.3.

For momenta much smaller than m_π , explicit pion exchange cannot be resolved such that these can be regarded as integrated out, much like we did explicitly for the pseudoscalar toy model in Sec. 2.2.3. The resulting “pionless” theory has, up to long-range forces that we consider in Sec. 5.1) only contact interactions between nucleons left. These contact interactions parameterize not only unresolved pion exchange, but also that of heavier mesons, for which contact terms already exist in Chiral EFT. Pionless EFT is formally very similar to the few-boson EFT discussed in Sec. 3, and it despite its simplicity it gives rise to surprisingly rich physics, as we will show in this section.

4.2 Pionless effective field theory

The neutron-proton S-wave scattering lengths are experimentally determined to be about 5.4 fm in the 3S_1 channel, and -23.7 fm in the 1S_0 channel. What is special about these numbers is that they are large compared to the typical nuclear length scale determined by the pion Compton wavelength, $m_\pi^{-1} \sim 1.4$ fm. This estimate comes from the long-range component of the nuclear interaction being determined by one-pion exchange. Naïvely, if we consider the low-energy limit (NN center-of-mass momentum going to zero) we expect that we can integrate out the pions and end up with a contact interaction scaling with the inverse pion mass, and thus a perturbative EFT reproducing natural-sized scattering lengths. The fact that this is not the case is typically interpreted as nature “choosing” the fine-tuned scenario outlined in Sec. 2.3.3. In this case, pion exchange¹⁷ combines with shorter range interactions to yield the large S-wave scattering lengths (and the deuteron as an unnaturally shallow bound state), implying that nuclear physics is a strongly coupled and thus nonperturbative system at low energies. This is what allows us to write down an EFT that is closely related to the one that describes strongly interacting bosons. What governs the physics of low-energy observables is to a good appropriation just the fact that the scattering lengths are large, so we end up with a short-range EFT much like the one for bosons encountered in Sec. 3. Some

¹⁷ As discussed in Sec. 5.3 this actually has to be the exchange of two or more pions, as one-pion exchange does not contribute to S-wave scattering at zero energy.

rather technical new features arise from the fact that nucleons are fermions with spin and isospin.

4.3 The two-nucleon S-wave system

The leading-order Lagrangian for pionless EFT can be written as

$$\mathcal{L} = N^\dagger \left(i\partial_0 + \frac{\nabla^2}{2M_N} + \dots \right) N - C_{0,s} (N^T \hat{P}_s N)^\dagger (N^T \hat{P}_s N) - C_{0,t} (N^T \hat{P}_t N)^\dagger (N^T \hat{P}_t N) + \dots, \quad (120)$$

with projectors

$$(\hat{P}_t)^i = \sigma^2 \sigma^i \tau^2 / \sqrt{8}, \quad (\hat{P}_s)^\lambda = \sigma^2 \tau^2 \tau^\lambda / \sqrt{8} \quad (121)$$

such that $C_{0,s}$ and $C_{0,t}$ refer to the 1S_0 and 3S_1 NN channels, respectively. As in previous sections of this chapter, we use σ^i to denote the Pauli matrices in spin space, and write $(\sigma^i)^\alpha_\beta$ to refer to their individual entries (with the upper index referring to the row). Conversely, we use the notation $(\tau^\lambda)^a_b$ in isospin space.

With the usual cartesian indices $i, \lambda = 1, 2, 3$ the projectors for given i or λ give somewhat unusual combinations of individual states. For example, np configurations are completely contained in the $\lambda = 3$ isospin component, whereas nn and pp are obtained from linear combinations $1 \pm i2$. In other words, in order to separate the physical states (and likewise to get spin-1 states with $m = 0, \pm 1$ quantum numbers) one should work instead with a spherical basis. For example, if one wants to include isospin-breaking terms, it is convenient to work with the projectors

$$(\tilde{P}_s)^{-1} = \frac{1}{\sqrt{2}} [(\hat{P}_s)^1 - i(\hat{P}_s)^2], \quad (\tilde{P}_s)^0 = (\hat{P}_s)^3, \quad (\tilde{P}_s)^{+1} = -\frac{1}{\sqrt{2}} [(\hat{P}_s)^1 + i(\hat{P}_s)^2]. \quad (122)$$

Otherwise, since the difference is a unitary rotation, the choice of basis is arbitrary.

4.3.1 Spin and isospin projection

To understand why the projectors have been defined as in Eq. (121), it is instructive to calculate the tree-level contribution to the amplitude in a given channel. With all spin and isospin vertices written out, the Feynman rule for the four-nucleon vertex in the 3S_1 channel is

$$\begin{array}{c} \delta, d \quad \alpha, a \\ \diagdown \quad \diagup \\ \bullet \\ \diagup \quad \diagdown \\ \gamma, c \quad \beta, b \end{array} \sim i \frac{C_{0,t}}{8} (\sigma^i \sigma^2)^\alpha_\beta (\tau^2)^a_b (\sigma^2 \sigma^i)^\gamma_\delta (\tau^2)^c_d, \quad (123)$$

which is obtained by simply writing out the $(\hat{P}_t)^i$ from Eq. (121). Furthermore, this diagram has an associated combinatorial factor 4 because there are two possibilities each to contract the in- and outgoing legs with external nucleon fields.

In order to calculate the T-matrix, we have to write out the Lippmann-Schwinger equation with all indices (and symmetry factors) and then apply the appropriate projectors. For 3S_1 and isospin 0, the result should have two free spin-1 indices, which we label k and j for the in- and outgoing side, respectively. The inhomogeneous term is just the vertex (123) with an additional factor 4. Applying the projectors, we get

$$\begin{aligned} & \frac{1}{\sqrt{8}} (\sigma^2 \sigma^j)^\beta_\alpha (\tau^2)^b_a \times 4 \times i \frac{C_{0,t}}{8} (\sigma^i \sigma^2)^\alpha_\beta (\tau^2)^a_b (\sigma^2 \sigma^i)^\gamma_\delta (\tau^2)^c_d \times \frac{1}{\sqrt{8}} (\tau^2)^d_c (\sigma^k \sigma^2)^\delta_\gamma \\ &= i \frac{C_{0,t}}{16} \text{Tr}(\sigma^j \sigma^i) \text{Tr}(\tau^2 \tau^2) \text{Tr}(\sigma^i \sigma^k) \text{Tr}(\tau^2 \tau^2) = i C_{0,t} \delta^{jk}, \end{aligned} \quad (124)$$

where we have used the well-known of the Pauli matrices. This is exactly the expected result: the projectors (121) have been constructed to give this. The projection of other, more complicated diagram works in the same way. Albeit somewhat tedious, it is technically straightforward. For higher partial waves, one of course has to take into account the coupling of spin and orbital angular momentum.

4.3.2 Dibaryon fields

Just like for bosons, it is convenient to introduce auxiliary dimer—now called dibaryon—field for each of the NN S-wave states. This is done by rewriting the Lagrangian (120) as

$$\begin{aligned} \mathcal{L} = & N^\dagger \left(i\partial_0 + \frac{\nabla^2}{2M_N} + \dots \right) - t^{i\dagger} \left[g_t + \left(i\partial_0 + \frac{\nabla^2}{4M_N} \right) \right] t^i + y_t \left[t^{i\dagger} (N^T P_t^i N) + \text{h.c.} \right] \\ & - s^{\lambda\dagger} \left[g_s + \left(i\partial_0 + \frac{\nabla^2}{4M_N} \right) \right] s^\lambda + y_s \left[s^{\lambda\dagger} (N^T P_s^\lambda N) + \text{h.c.} \right] + \dots, \end{aligned} \quad (125)$$

where t (s) denotes a 3S_1 (1S_0) dibaryon field and the projection operators $P_{s,t}$ are as defined in Eq. (121). The “bare” dibaryon propagators are just $i/g_{s,t}$, while the full leading-order expressions are obtained by summing up all nucleon bubble insertions. This resummation, which without dibaryon fields gives the NN T-matrix as a bubble chain, reflects the fact we need to generate shallow states (the bound deuteron and the virtual 1S_0 state) to account for the unnaturally large NN scattering lengths. Pionless EFT is designed to capture this feature.

Omitting spin-isospin factors for simplicity, the resummed propagators are

$$i\Delta_{s,t}(p_0, \mathbf{p}) = \frac{-i}{g_{s,t} + y_{s,t}^2 I_0(p_0, \mathbf{p})}, \quad (126)$$

where

$$I_0(p_0, \mathbf{p}) = M_N \int^\Lambda \frac{d^3q}{(2\pi)^3} \frac{1}{M_N p_0 - \mathbf{p}^2/4 - \mathbf{q}^2 + i\epsilon} = -\frac{M_N}{4\pi} \left(\frac{2\Lambda}{\pi} - \sqrt{\frac{\mathbf{p}^2}{4} - M_N p_0 - i\epsilon} \right) + \mathcal{O}(1/\Lambda) \quad (127)$$

is the familiar bubble integral regularized with a momentum cutoff. The cutoff dependence is absorbed into the parameters $y_{s,t}$ and $g_{s,t}$ to obtain the renormalized propagators. Attaching external nucleon legs gives the NN T-matrix,

$$iT_{s,t}(k) = (iy_{s,t})^2 i\Delta_{s,t}(p_0 = k^2/M_N, \mathbf{p} = \mathbf{0}) = \frac{4\pi}{M_N} \frac{i}{k \cot \delta_{s,t}(k) - ik}, \quad (128)$$

so we can match to the effective range expansions for $k\delta_{s,t}(k)$. At leading order, the renormalization condition is to reproduce $k \cot \delta_{s,t}(k) = -1/a_{s,t} + \mathcal{O}(k^2)$, which gives

$$\frac{4\pi g_{s,t}}{M_N y_{s,t}^2} = -\frac{1}{a_{s,t}} + \frac{2\Lambda}{\pi}. \quad (129)$$

Instead of this standard choice of the expansion around the zero-energy threshold, it is convenient to expand the 3S_1 channel around the deuteron pole.¹⁸ This is

$$k \cot \delta_t(k) = \gamma_t + \frac{\rho_t}{2} (k^2 + \gamma_t^2) + \dots, \quad (130)$$

where $\gamma_t = \sqrt{M_N B_d} \simeq 45.7$ is the deuteron binding momentum and $\rho_t \simeq 1.765$ is the “deuteron effective range.” This choice, which sets

$$\frac{4\pi g_t}{M_N \gamma_t^2} = -\gamma_t + \frac{2\Lambda}{\pi}, \quad (131)$$

gets the exact deuteron pole position right at leading order, but is equivalent to the choice in Eq. (129) up to range corrections.

Wavefunction renormalization

The residue at the deuteron pole gives the deuteron wavefunction renormalization. We find

$$Z_t^{-1} = i \frac{\partial}{\partial p_0} \frac{1}{i\Delta_t(p_0, \mathbf{p})} \Big|_{p_0 = -\frac{\gamma_t^2}{M_N}, \mathbf{p}=0} = \frac{M_N^2 \gamma_t^2}{8\pi \gamma_t} \Rightarrow \sqrt{Z_t} = \frac{1}{\gamma_t} \frac{\sqrt{8\pi \gamma_t}}{M_N} \quad (132)$$

for the renormalization as in Eq. (131). If we directly consider the (off-shell) T-matrix near the pole, we find

$$\begin{aligned} T(E) &= \frac{4\pi}{M_N - \gamma_t + \sqrt{-M_N E - i\varepsilon}} = -\frac{4\pi}{M_N} \frac{\sqrt{-M_N E - i\varepsilon} + \gamma_t}{-M_N E - \gamma_t^2} \quad \text{for } \varepsilon \rightarrow 0 \\ &\sim -\frac{8\pi \gamma_t}{M_N^2} \frac{1}{E + \frac{\gamma_t^2}{M_N}} \quad \text{as } E \rightarrow -\gamma_t^2/M_N. \end{aligned} \quad (133)$$

Comparing to the standard factorization at the pole,¹⁹

$$T(k, p; E) = -\frac{B^\dagger(k)B(p)}{E + E_B} + \text{terms regular at } E = -E_B, \quad (134)$$

we can read off from Eq. (133) that

$$B(p) = \sqrt{\frac{8\pi \gamma_t}{M_N^2}} = \gamma_t \sqrt{Z_t}, \quad (135)$$

independent of momentum at this order.

4.4 Three nucleons: scattering and bound states

As done in Sec. 3.3 for bosons, the dimer/dibaryon formalism allows for a particularly intuitive and simple description of the three-body system. Looking at nucleon-deuteron S-wave

¹⁸ The shallow deuteron bound-state pole is within the radius of convergence of the effective range expansion. The deuteron binding momentum is $\gamma_t = 1a_t + \dots$, where the ellipses include corrections from the effective range (and higher-order shape parameters).

¹⁹ The minus sign in Eq. (134) is a consequence of the convention we use here for the T-matrix.

scattering²⁰, we find that the spin 1 of the deuteron can couple with the spin 1/2 of the nucleon to a total spin of either 3/2 or 1/2. These two cases are referred to as the quartet and doublet channel, respectively.

4.4.1 Quartet channel

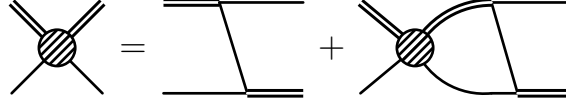


Fig. 11 Nd quartet-channel integral equation. Nucleons and deuterons are represented as single and double lines, respectively. The blob represents the T-matrix.

In the quartet-channel, the spins of all three nucleons have to be aligned to produce the total spin 3/2. This means that only the deuteron field can appear in intermediate states, and the Pauli principle excludes a three-body contact interaction without derivatives. The resulting integral equation for the Nd T-matrix is shown diagrammatically in Fig. 11. Compared to Fig. 8, we use a different convention here where the T-matrix blob is drawn to the left of the nucleon exchange, and we denote in- and outgoing momenta (in the Nd center-of-mass frame) by $\pm \mathbf{k}$ and $\pm \mathbf{p}$, respectively.²¹ The energy and momentum dependence are exactly the same as for bosons, but we have to include the additional spin-isospin structure from the vertices. Doing this, the result in its full glory reads:

$$\begin{aligned}
 (iT_q^{ij})^{\beta b}_{\alpha a}(\mathbf{k}, \mathbf{p}; E) = & -\frac{iM_N y_I^2}{2} (\sigma^j \sigma^i)^{\beta}_{\alpha} \delta_a^b \frac{1}{\mathbf{k}^2 + \mathbf{k} \cdot \mathbf{p} + \mathbf{p}^2 - M_N E - i\epsilon} \\
 & + \int \frac{d^3 q}{(2\pi)^3} \Delta_t \left(E - \frac{\mathbf{q}^2}{2M_N}, \mathbf{q} \right) (iT_q^{ik})^{\gamma c}_{\alpha a}(E; \mathbf{k}, \mathbf{q}) \\
 & \times \frac{M_N y_I^2}{2} \frac{(\sigma^j \sigma^k)^{\beta}_{\gamma} \delta_c^b}{\mathbf{q}^2 + \mathbf{q} \cdot \mathbf{p} + \mathbf{p}^2 - M_N E - i\epsilon}. \quad (136)
 \end{aligned}$$

This unprojected amplitude carries spin and isospin indices for the various fields in the initial and final states. To select the overall spin 3/2 contribution, we take linear combinations as in Eq. (122) to select the maximal projections for the in- and outgoing deuterons and $\alpha = \beta = 1$ to get nucleons with spin orientation $+1/2$. We also set $a = b = 2$ to select neutrons. Altogether, this gives

$$(\sigma^j \sigma^i)^{\beta}_{\alpha} \delta_a^b \rightarrow 2, \quad (137)$$

in the inhomogeneous term, and the same factor for the integral part. The fully projected quartet-channel amplitude is

$$T_q = \frac{1}{2} (T_q^{11} + i(T_q^{12} - T_q^{21}) + T_q^{22})_{12}^{12}. \quad (138)$$

7. Exercise: Work out the details leading to Eq. (138).

Finally, the S-wave projection of Eq. (136) is done by applying the operator $\frac{1}{2} \int_{-1}^1 d\cos \theta$, where θ is the angle between \mathbf{k} and \mathbf{p} . Introducing a momentum cutoff Λ , the resulting equation

²⁰ We work in the isospin-symmetric theory here, but in the absence of electromagnetic interactions (discussed in Sec. 5.1), the nucleon here should be thought of as a neutron.

²¹ Unlike what is done in Sec. 3, we also read diagrams from left (incoming particles) to right (outgoing particles). Both conventions can be found in the literature.

tion can be solved numerically by discretizing the remaining one-dimensional integral. From the result, which we denote by T_q^0 , we can calculate observables like scattering phase shifts,

$$\delta_q(k) = \frac{1}{2i} \ln \left(1 + \frac{2ikM_N}{3\pi} Z_t T_q^0(k, k; E_k) \right), \quad E_k = \frac{3k^2}{4M_N} - \frac{\gamma_t^2}{M_N}, \quad (139)$$

or the Nd scattering length:

$$a_q = \frac{M_N}{3\pi} \lim_{k \rightarrow 0} Z_t T_q^0(k, k; E_k). \quad (140)$$

Note that we have not absorbed the wavefunction renormalization Z_t into T_q^0 but instead chose to keep it explicit in Eqs. (139) and (140)

4.4.2 Doublet channel

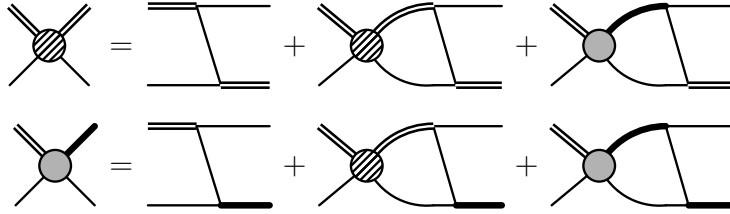


Fig. 12 Nd doublet-channel integral equation. As in Fig. 11, nucleons and deuterons are drawn as single and double lines, respectively. Additionally, we represent the 1S_0 dibaryon as a thick line. The hatched and shaded blobs are the two components of the doublet-channel $Nd \rightarrow Nd$ T-matrix.

The doublet channel (total spin 1/2) has a richer structure, since now also the 1S_0 dibaryon can appear as an intermediate state. The result is a coupled channel integral equation, shown diagrammatically in Fig. 12. We skip here the technicalities of the spin-isospin projection (for details, see Ref. [28] and earlier references therein) and merely quote the result in a compact notation:

$$\begin{pmatrix} T_{d,1}^0 \\ T_{d,2}^0 \end{pmatrix} = \begin{pmatrix} M_N y_t^2/2 \\ -3M_N y_t y_s/2 \end{pmatrix} K + \begin{pmatrix} D_t & 0 \\ 0 & D_s \end{pmatrix} \begin{pmatrix} -M_N y_t^2/2 & 3M_N y_t y_s/2 \\ 3M_N y_s y_t/2 & -M_N y_s^2/2 \end{pmatrix} K \otimes \begin{pmatrix} T_{d,1}^0 \\ T_{d,2}^0 \end{pmatrix}, \quad (141)$$

where K is the “kernel” function

$$K(k, p; E) = \frac{1}{2kp} \ln \left(\frac{k^2 + p^2 + kp - M_N E - i\epsilon}{k^2 + p^2 - kp - M_N E - i\epsilon} \right), \quad (142)$$

$$EFT - D_{s,t}(q; E) = \Delta_{s,t} \left(E - \frac{q^2}{2M_N}; q \right), \quad (143)$$

and the integral operation

$$A \otimes B \equiv \frac{1}{2\pi^2} \int_0^\Lambda dq q^2 A(\dots, q) B(q, \dots) \quad (144)$$

has to be applied within each block. Just like the quartet-channel equation, Eq. (141) can be solved numerically by discretizing the integrals, with the additional complication that we now

have a 2×2 block matrix. The T-matrix likewise becomes a 2-block vector, the upper part of which gives the physical $Nd \rightarrow Nd$ amplitude.²²

8. Exercise: Express the fully projected integral equation for the quartet channel amplitude T_q^0 using the compact notation based on Eqs. (142), (143), and (144).

Leading-order three-nucleon force

Studying the doublet-channel solution as a function of increasing UV cutoff Λ , one finds that there is no stable limit as $\Lambda \rightarrow \infty$. Instead, the amplitude changes wildly as Λ is varied. This is much unlike the quartet-channel case, which shows a rapid convergence with Λ .

The origin of this behavior was explained by Bedaque *et al.* [29]. The behavior for large Λ is governed by large momenta, which means that infrared scales like the scattering lengths do not matter. Indeed, one finds that $D_t(E; q)$ and $D_s(E; q)$ have the same leading behavior as $q \rightarrow \infty$. To analyze the asymptotic behavior of the amplitude we can thus go to the $SU(4)$ spin-isospin symmetric limit and set $D_t = D_s \equiv D$ as well as $y_t = y_s \equiv y$. In this limit, the two integral equations in Eq. (141) can be decoupled by defining $T_{d,\pm} = T_{d,1} \pm T_{d,2}$. For $T_{d,+}$ we find the integral equation

$$T_{d,+}^0(k, p; E) = -M_N y^2 K(k, p; E) + M_N y^2 \int_0^\Lambda \frac{dq}{2\pi^2} q^2 K(k, q; E) D(q; E) T_{d,+}^0(q, p; E), \quad (145)$$

which is formally exactly the same as the three-boson integral equation, Eq. (101), in the absence of a three-body force. As discussed in Sec. 3.3, this equation does not have a unique solution in the limit $\Lambda \rightarrow \infty$. Since $T_{d,1/2}$ are linear combinations of involving $T_{d,+}$, they inherit the same behavior. But the cure is now obvious: a three-nucleon force, which by naïve counting would only enter at higher orders, has to be promoted to leading order in order to make Eq. (141) well defined. This three-nucleon force, like the asymptotic amplitudes, is $SU(4)$ symmetric (invariant under arbitrary spin-isospin rotations) and can be written as

$$\mathcal{L}_3 = \frac{h_0}{3} N^\dagger \left[y_t^2 t^{i\dagger} t^j \sigma^i \sigma^j + y_s^2 s^{A\dagger} s^B \tau^A \tau^B - y_t y_s (t^{i\dagger} s^A \sigma^i \tau^A + \text{h.c.}) \right] N, \quad (146)$$

where the cutoff-running of the three-nucleon coupling is analogous to what we derived for bosons:

$$h_0 = \frac{M_N H(\Lambda)}{\Lambda^2}. \quad (147)$$

Including this, the coupled doublet-channel integral equation becomes

$$\begin{pmatrix} T_{d,1}^0 \\ T_{d,2}^0 \end{pmatrix} = \begin{pmatrix} M_N y_t^2 / 2 \\ -3M_N y_t y_s / 2 \end{pmatrix} K + \begin{pmatrix} D_t & 0 \\ 0 & D_s \end{pmatrix} \begin{pmatrix} -M_N y_t^2 / 2(K + h_0) & 3M_N y_t y_s / 2(K + h_0) \\ 3M_N y_s y_t / 2(K + h_0) & -M_N y_s^2 / 2(K + h_0) \end{pmatrix} \otimes \begin{pmatrix} T_{d,1}^0 \\ T_{d,2}^0 \end{pmatrix}. \quad (148)$$

We stress that the requirement to include this three-body force at leading-order is a feature of the nonperturbative physics that can be traced back to the large NN scattering lengths. All loop diagrams obtained by iterating the integral equation are individually finite as $\Lambda \rightarrow \infty$, yet their infinite sum does not exist in that limit unless the h_0 contact interaction is included.

²² Note that this vector is one part of the more general full off-shell amplitude, which is a 2×2 block matrix including the two combinations of dibaryon legs that do not appear in Fig. 12.

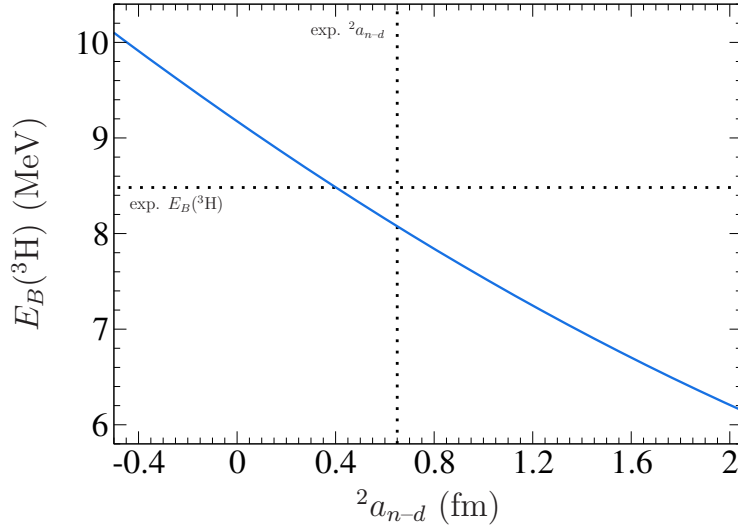


Fig. 13 Correlation (Phillips line) between ${}^3\text{H}$ binding energy (in MeV) and doublet nd scattering length (in fm) in leading-order pionless EFT.

The Phillips line

The form of $H(\Lambda)$ is given by Eq. (118), but since there is a prefactor that depends on the details of the regularization scheme, in practice one has to determine the appropriate value numerically after choosing a cutoff Λ . This requires a three-body datum as input, which is conveniently chosen to be the triton binding energy—the ${}^3\text{H}$ bound state corresponds to a pole in T_d at $E = -E_B({}^3\text{H})$, *cf.* Sec. 3.4—or the doublet-channel nd scattering length (or, in principle, a phase shift at some fixed energy). Once one of these is fixed, the rest can be predicted. In particular, this means that the existence of a single three-body parameter in pionless EFT at leading order provides a natural explanation of the Phillips line, *i.e.*, the observation that various phenomenological potentials, which were all tuned to produce the same NN phase shifts, gave different results for the triton binding energy and doublet S-wave scattering length, which however are strongly correlated. In our framework, we can obtain the line shown in Fig. 13 by fitting $H(\Lambda)$ to different values of the scattering length and then calculating $E_B({}^3\text{H})$ (or vice versa). Alternatively, one can find the same curve by setting h_0 to zero and varying Λ to move along the line.

With this, we conclude our discussion the three-nucleon system. For more details, like calculations beyond leading order, we encourage the reader to encourage the literature.

5 Beyond short-range interactions: adding photons and pions

5.1 Electromagnetic interactions

So far, we have studied only effective theories where the particles (atoms or nucleons) interact solely via short-range force (regulated contact interactions). While this is, as we have argued, sufficient to describe the strong nuclear interactions at (sufficiently low) energies where the EFT is valid, the electromagnetic interaction does not fit in this scheme. Nevertheless, since almost all systems of interest in low-energy nuclear physics involve more than one proton, the inclusion of such effects is of course important.

Any coupling of photons to charged particles has to be written down in a gauge-invariant way. A natural way to ensure gauge invariance is to replace all derivatives in the effective Lagrangian with covariant ones, *i.e.*,

$$\partial_\mu \rightarrow D_\mu = \partial_\mu + ieA_\mu \hat{Q}, \quad (149)$$

where \hat{Q} is the charge operator (for nucleons, for example, $\hat{Q}_N = (\mathbf{1} + \tau_3)/2$). Moreover $e^2 = 4\pi\alpha$ defines the electric unit charge in terms of the fine structure constant $\alpha \approx 1/137$.

Since in the EFT there is an infinite tower of contact interactions with an increasing number of derivatives, we also get an infinite number of photon vertices. Still, merely plugging in the covariant derivative is not enough (after all, this is called *minimal* substitution); it is possible to write down terms which are gauge invariant by themselves, and for the EFT to be complete these have to be included as well. Before we come back to this in Sec. 5.1.4, let us first see what we get from gauging the derivatives in the nucleon kinetic term:

$$N^\dagger \left(i\partial_t + \frac{\nabla^2}{2M_N} + \dots \right) N \rightarrow N^\dagger \left(iD_t + \frac{\mathbf{D}^2}{2M_N} + \dots \right) N. \quad (150)$$

In addition to this, we also have to include the photon kinetic and gauge fixing terms to complete the electromagnetic sector. A convenient choice for the our nonrelativistic framework is Coulomb gauge, *i.e.*, demanding that $\nabla \cdot \mathbf{A} = 0$. A covariant way to write this condition is

$$\partial_\mu A^\mu - \eta_\mu \eta_\nu \partial^\nu A^\mu = 0 \quad (151)$$

with the timelike unit vector $\eta^\mu = (1, 0, 0, 0)$. Hence, we add to our effective Lagrangian the term

$$\mathcal{L}_{\text{photon}} = -\frac{1}{4} F_{\mu\nu} F^{\mu\nu} - \frac{1}{2\xi} (\partial_\mu A^\mu - \eta_\mu \eta_\nu \partial^\nu A^\mu)^2. \quad (152)$$

5.1.1 The Coulomb force

From Eq. (152) we get the equation of motion for the photon field as

$$\left[\square g^{\mu\nu} - \partial^\mu \partial^\nu + \frac{1}{\xi} \left(\partial^\mu \partial^\nu - \eta^\nu \eta_\kappa \partial^\mu \partial^\kappa - \eta^\mu \eta_\lambda \partial^\lambda \partial^\nu + \eta^\mu \eta^\nu \eta_\lambda \eta_\kappa \partial^\lambda \partial^\kappa \right) \right] A_\nu(x) = 0. \quad (153)$$

The photon propagator is defined as the Feynman Green's function for the differential operator acting on $A_\nu(x)$. Writing down the general solution in momentum space and choosing $\xi = 0$ at the end (recall that it is an artificial parameter introduced through enforcing the gauge condition in the path integral [30]), we get

$$D_\gamma^{\mu\nu}(k) = \frac{-i}{k^2 + i\epsilon} \left(g^{\mu\nu} + \frac{k^\mu k^\nu + k^2 \eta^\mu \eta^\nu - (k \cdot \eta)(k^\mu \eta^\nu + \eta^\mu k^\nu)}{(k \cdot \eta)^2 - k^2} \right). \quad (154)$$

A simple inspection of which shows that it vanishes if μ or $\nu = 0$. In other words, A_0 photons do not propagate. Correspondingly, their equation of motion becomes time independent and we can use it to remove A_0 from the effective Lagrangian (the nuclear part plus $\mathcal{L}_{\text{photon}}$). We find

$$\nabla^2 A_0 = -eN^\dagger \hat{Q}N, \quad (155)$$

which is just the Poisson equation with the nucleon charge density on the right-hand side. Solving this in Fourier space, where ∇^2 turns into the squared three-momentum, we eventually get a term

$$\mathcal{L}_{\text{Coulomb}}(x_0, \mathbf{x}) = -e^2 \int d^3y N^\dagger(x_0, \mathbf{x}) N(x_0, \mathbf{x}) \frac{e^{-i\mathbf{q} \cdot (\mathbf{x}-\mathbf{y})}}{\mathbf{q}^2} \left(\frac{1+\tau^3}{2} \right) N^\dagger(x_0, \mathbf{y}) N(x_0, \mathbf{y}), \quad (156)$$

i.e., static Coulomb potential ($\sim 1/r$ in configuration space) between charged nucleons. This is a non-local interaction that really should be kept in the Lagrangian as a whole. Still, to calculate Feynman diagrams it is convenient to split it up into a vertex

$$\begin{array}{c} \beta, b, \mathbf{q} \quad \quad \alpha, a, \mathbf{q} + \mathbf{k} \\ \quad \quad \quad \diagdown \quad \diagup \\ \quad \quad \quad \text{---} \quad \text{---} \\ \quad \quad \quad \diagup \quad \diagdown \\ \quad \quad \quad 0, \mathbf{k} \end{array} \quad \sim -ie \left(\frac{1+\tau^3}{2} \right)_b^a \delta^\alpha_\beta, \quad (157)$$

and a factor i/\mathbf{k}^2 for each “Coulomb-photon propagator,” which is really just an expression for the static potential in momentum space. Note that the sign in Eq. (157) is arbitrary because these vertices really only come in pairs; we have chosen it here to coincide with what one would naïvely read off from the $N^\dagger iD_0 N$ term.

Finding that A_0 photons only appear as static internal exchanges goes well in line that physical photons in external states have to be transverse. Still, one might wonder how to treat diagrams with virtual photons coupled to a nuclear system (*e.g.*, electrodisintegration), which should have A_0 contributions. The answer is that the proper way to treat these is to add appropriate external currents to the Lagrangian, which then, in turn, appear on the right-hand side of Eq. (155).

5.1.2 Coulomb enhancement and divergences

The Coulomb force is a long-range interaction: it only falls off like a power law ($\sim 1/r$) in configuration space. In momentum space, it correspondingly has a pole at vanishing momentum transfer ($\mathbf{q}^2 = 0$), *i.e.*, it gives rise to an infrared divergence. There are standard techniques for dealing with this, for example defining so-called Coulomb-modified scattering phase shifts and effective-range expansions well-known from quantum-mechanical scattering theory. These are based on treating Coulomb effects fully nonperturbatively, *i.e.*, resumming to exchange of Coulomb photons to all orders. In the EFT power counting, the need for this resummation is reflected in the fact dressing a given two-body scattering diagram with external momenta of order Q by an additional Coulomb photon gives a factor $\alpha M_N/Q$, *i.e.*, an *enhancement* if $Q \lesssim \alpha M_N$. In Figure 14 we show this for two-photon exchange compared to the single-photon diagram.

$$\begin{array}{c} \text{---} \\ | \\ \text{---} \end{array} \sim \frac{\alpha}{Q^2} \quad \begin{array}{c} \text{---} \\ | \\ \text{---} \\ | \\ \text{---} \end{array} \sim \frac{Q^5}{M_N} \left(\frac{\alpha}{Q^2} \right)^2 \left(\frac{M_N}{Q^2} \right)^2 = \frac{\alpha}{Q^2} \times \frac{\alpha M_N}{Q}$$

Fig. 14 Infrared enhancement of Coulomb-photon exchange.

If a problem with Coulomb interactions is solved numerically, the IR divergence has to be regularized in some way to have all quantities well defined. One way to do this “screening” the potential with a photon mass λ , *i.e.*, replacing \mathbf{q}^2 with $\mathbf{q}^2 + \lambda^2$ in the Coulomb-photon propagator. If this is done, λ should be kept as small as possible and be extrapolated to zero for all physical observables at the end of the calculation.

In contrast to what one might naïvely expect, Coulomb contributions can also modify the UV behavior of diagrams. Consider, for example the insertion of a single photon within a bub-

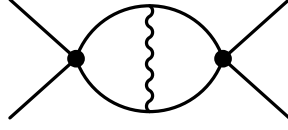


Fig. 15 Single photon insertion in a proton-proton bubble diagram.

ble contributing to proton-proton scattering, as shown in Fig. 15. Power counting momenta in this diagram (with C_0 vertices) gives a factor $(Q^5/M_N)^2$ from the two loops, $(M_N/Q^2)^4$ from the nucleon propagators, and an obvious α/Q^2 from the photon, meaning that overall we have Q^0 , corresponding to a superficial logarithmic divergence of this diagram (which one can confirm with an explicit calculation). This is a new feature compared to the theory with only short-range interactions, where this particular divergence is absent (all divergences are of power-law type there). Without going into any details, we stress that this divergence has to be accounted for when the theory with Coulomb contributions is renormalized. In particular, this example teaches us that in the EFT the Coulomb force is not merely an “add-on potential” that slightly shifts results, but that it has to be treated consistently along with the short-range interactions.

5.1.3 Transverse photons

Transverse photons come from the quadratic spatial derivative:

$$\mathbf{D}^2 = (\partial^i + ieA^i\hat{Q})(\partial^i + ieA^i\hat{Q}) = \nabla^2 + ie(A^i\hat{Q}\partial^i + \partial^i A^i\hat{Q}) - e^2 A^2 \hat{Q}. \quad (158)$$

We can rewrite this using

$$\partial^i (A^i \hat{Q} N) = (\partial^i A^i) \hat{Q} N + A^i \hat{Q} \partial^i N, \quad (159)$$

where the first term vanishes in Coulomb gauge. Hence, we get the vertex

$$\begin{array}{c} \beta, b, \mathbf{q} \\ \diagdown \quad \diagup \\ \text{---} \quad \text{---} \\ \diagup \quad \diagdown \\ n, \mathbf{k} \end{array} \quad \begin{array}{c} \alpha, a, \mathbf{q} + \mathbf{k} \\ \diagup \quad \diagdown \\ \text{---} \quad \text{---} \\ \diagdown \quad \diagup \end{array} \quad \sim -\frac{e}{M_N} \left(\frac{\mathbf{1} + \boldsymbol{\tau}^3}{2} \right)_b^a \delta^\alpha_\beta (i\mathbf{q})^n, \quad (160)$$

with the momentum dependence coming from the derivative. We leave it as an exercise to write down the Feynman rule for the two-photon term $\sim A^2 \hat{Q}$.

Comparing Eq. (160) with Eq. (157) that a diagram with the exchange of a transverse photon is suppressed by a factor Q^2/M_N^2 compared to the same topology with a Coulomb photon. Transverse photons also have a more complicated propagator than the simple i/\mathbf{k}^2 that we found for Coulomb photons. From Eq. (154) we find that

$$m \text{ --- } (k_0, \mathbf{k}) \text{ --- } n \sim \frac{i}{k_0^2 - \mathbf{k}^2 + i\epsilon} \left(\delta^{mn} - \frac{k^m k^n}{\mathbf{k}^2} \right). \quad (161)$$

which now depends on the energy k_0 and thus gives rise to poles in Feynman diagrams. Note that the structure is somewhat different from what one typically sees in QED textbooks that use Lorenz/Feynman gauge.

The covariant derivative alone only gives us photons coupled to the proton's charge. However, as mentioned previously, minimal substitution only gives a subset of all possible electromagnetic terms. For example, the magnetic coupling of photons to the nucleons (both protons and neutrons in this case) is given by

$$\mathcal{L}_{\text{mag}} = \frac{e}{2M_N} N^\dagger (\kappa_0 + \kappa_1 \tau^3) \vec{\sigma} \cdot \mathbf{B} N. \quad (162)$$

where κ_0 and κ_1 are the isoscalar and isovector nucleon magnetic moments, respectively. That is, the low-energy constant of this operator has been fixed directly to the associated single-nucleon observable (similarly to how the nucleon mass is fixed immediately in the nonrelativistic theory). With $\mathbf{B} = \nabla \times \mathbf{A}$ and all indices written out, this is

$$\mathcal{L}_{\text{mag}} = \frac{e}{2M_N} N_{\alpha a}^\dagger (\kappa_0 \mathbf{1} + \kappa_1 \tau^3)^a_b (\boldsymbol{\sigma}^i)^\alpha_\beta \varepsilon_{ijm} \partial^j A^m N^{\beta b}. \quad (163)$$

and it gives rise to the Feynman rule

$$\begin{array}{c} \beta, b \\ \diagdown \\ \text{---} \\ \diagup \\ \alpha, a \end{array} \sim \frac{ie}{2M_N} (\kappa_0 \mathbf{1} + \kappa_1 \tau^3)^a{}_b \varepsilon_{ijm} (\sigma^i)^\alpha{}_\beta (\mathbf{i}\mathbf{k})^j. \quad (164)$$

We point out that Eq. (163) only gives the leading magnetic coupling. In traditional nuclear physics language, it corresponds to a one-body operator. At higher orders in the EFT, there are additional operators, like a four-nucleon contact interaction with an additional photon. Such many-body terms correspond to what phenomenological approaches model as “meson exchange currents.”

5.2 Example: deuteron breakup

As an application of the things discussed in the previous sections, we now consider the low-energy reaction $d\gamma \leftrightarrow np$. By time-reversal symmetry, the amplitudes for the processes corresponding to the two possible directions of the arrow are the same. For definiteness, we show the simplest diagram for the breakup reaction in Fig. 16.

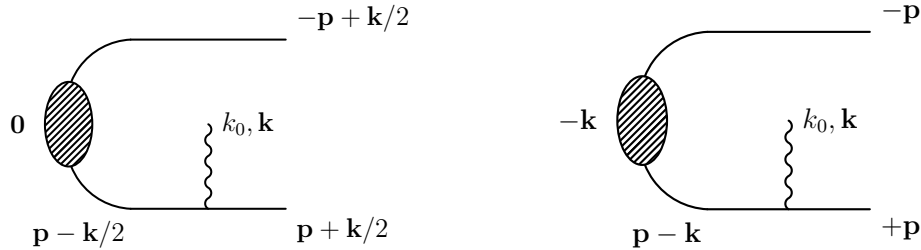


Fig. 16 Deuteron breakup diagram in two different kinematic frames. **Left:** lab frame, deuteron at rest. **Right:** center-of-mass frame of the outgoing nucleons.

The reaction can be considered in different reference frames. In the lab frame (left panel of Fig. 16), the deuteron is initially at rest and then gets hits by a photon with four-momentum (k_0, \mathbf{k}) . For our theoretical discussion here it is more convenient to take the two outgoing

nucleons in their center-of-mass frame, as shown in the right panel of Fig. 16). To first order, we can translate between the two frames by boosting all nucleons lines with a momentum $\mathbf{k}/2$. A more careful analysis would keep track of relativistic kinematics (the external photon is never nonrelativistic), but this is not essential for the illustration here, so we can get away with interpreting (k_0, \mathbf{k}) to mean different things in the two frames.

In the NN center-of-mass frame, the initial and final-state energies are

$$E_i = k_0 + \frac{k^2}{4M_N} - \frac{\gamma_t^2}{M_N}, \quad (165a)$$

$$E_f = \frac{p^2}{2M_N} + \frac{p^2}{2M_N} = \frac{p^2}{M_N}, \quad (165b)$$

where we have neglected the small deuteron binding energy by setting $M_d = 2M_N$. Conservation of energy implies that

$$p = \sqrt{M_N k_0 - \gamma_t^2 + k^2/4} \Leftrightarrow k_0 = \frac{p^2}{M_N} - \frac{k^2}{4M_N} + \frac{\gamma_t^2}{M_N}, \quad (166)$$

and the energy assigned to the internal nucleon propagator has to be $-\frac{k_0}{2} - \frac{\gamma_t^2}{2M_N} + \frac{k^2}{8M_N}$.

The blob in Fig. 16 represents the deuteron vertex function calculated in Sec. 4.3.2. Taking the result found there and adding the spin-isospin structure, we find

$$i \begin{array}{c} \beta, b \\ \diagup \\ \text{blob} \\ \diagdown \\ \alpha, a \end{array} \sim i \frac{1}{\sqrt{8}} \frac{\sqrt{8\pi\gamma_t}}{M_N} (\sigma^i \sigma^2)^\alpha{}_\beta (\tau_2)^a{}_b. \quad (167)$$

With this, we can finally write down the amplitude. For an E1 transition, the photon couples to the nucleon charge via the Feynman rule given in Eq. (160). Combining this with the ingredients above, we get

$$\begin{aligned} i\mathcal{M}_{E1} &= 2 \times \frac{-e}{M_N} \left(\frac{\mathbf{1} + \boldsymbol{\tau}^3}{2} \right)_a^c \delta_\alpha^\gamma i(\mathbf{p} - \mathbf{k})^j \frac{i}{-\frac{k_0}{2} - \frac{\gamma_t^2}{2M_N} + \frac{k^2}{8M_N} - \frac{(\mathbf{p} - \mathbf{k})^2}{2M_N} + i\epsilon} \frac{i}{\sqrt{8}} \frac{\sqrt{8\pi\gamma_t}}{M_N} (\sigma^2 \sigma^i)^\beta{}_\gamma (\tau_2)^b{}_c \\ &\quad \times (\epsilon_{s_\gamma}^*)^j (\epsilon_{s_d}^*)^i (N_{s_p})^{\alpha a} (N_{s_n})_{\beta b}. \end{aligned} \quad (168)$$

We have included a factor 2 to account for the fact that in drawing the diagram, the photon could be coupled to either nucleon (the isospin projection operator ensures of course that only the proton charge gives a contribution). Moreover, in the second line we have included polarization vectors and spinors for all external particles, the spins of which we denote as s_γ , s_d , s_p , and s_n , respectively. From the amplitude in Eq. 168 one can proceed to calculate the corresponding cross section by summing/averaging over the various initial and final states and integrating over the available phase space. We skip these details and close by noting that the isospin part is of course completely fixed (“polarized”) by the experimental setup. Hence, the spinor-isospinors are

$$(N_{s_p})^{\alpha a} = N_{s_p}^\alpha \begin{pmatrix} 1 \\ 0 \end{pmatrix}^a, \quad (N_{s_n})_{\beta b} = N_{s_p}^\alpha \begin{pmatrix} 1 \\ 0 \end{pmatrix}_b, \quad (169)$$

i.e., we can directly set $a = 1$ (isospin “up”, proton) and $b = 2$ (isospin “down”, neutron) in the amplitude.

9. Exercise: Write down the analog of Eq. (168) with a magnetically-coupled (M1) photon.

5.3 Chiral effective field theory

Pionless EFT provides a simple yet powerful framework to describe few-nucleon systems at very low energies, but its name implies its natural limitation, *i.e.*, the inability to describe physics at energy scales where pion exchange can be resolved. Certainly this becomes important for scattering calculations at momentum scales larger than the pion mass. But nuclear binding also generally increases with increasing number A of bound nucleons, which translates to larger typical momentum scales within the nucleus. There are indications that pionless EFT still converges for $A = 4$, but the question is not fully settled.

The construction of an effective field theory of nucleons and pions was pioneered by Weinberg in the early 1990s [31, 32], proposing a scheme to construct a nuclear potential based on Feynman diagrams from chiral perturbation theory. This theory, which is constructed as an expansion around the so-called “chiral limit,” in which the pions are exactly massless Goldstone bosons. The resulting theory, which has been applied with great success in the purely pionic and single-nucleon sector, treats the pion mass as a *small* scale and thus has a power counting designed for typical momenta $Q \sim m_\pi$.

For two or more nucleons, the theory is highly nonperturbative, which motivated Weinberg to develop a scheme where the power counting is applied to the *potential* instead of the amplitude, as we have otherwise done throughout this section. Kaplan *et al.* [17, 33, 34] proposed a different scheme where pions are included perturbatively on top of a leading order given by pionless EFT. This approach has, however, been found not to converge in channels where pion exchange generates a singular attractive interaction [35]. It is thus understood today that pions in general have to be treated nonperturbatively, in a framework generally referred to as “chiral effective field theory.” How exactly this should be implemented, however, is still a matter of debate. Instead of summarizing this here, we refer the reader to the literature (see, e.g., Refs. [13, 36–43]).

5.3.1 Leading-order pion-nucleon Lagrangian

For a thorough introduction to the field of chiral perturbation theory, we recommend the reader to study the lecture notes of Scherer and Schindler [44] as well as the vast original literature cited therein. It uses an elaborate formalism to construct the most general pion-nucleon Lagrangian that is invariant under chiral transformations (individual rotations of left- and right-handed nucleon fields) plus terms implementing the explicit breaking of chiral symmetry due to finite quark masses. In the conventions of Ref. [44], the leading-order pion-nucleon Lagrangian is

$$\mathcal{L}_{\pi N}^{(1)} + \mathcal{L}_2^\pi = \bar{\psi} \left(i \not{D} - M_N + \frac{g_A}{2} \gamma^\mu \gamma^5 u_\mu \right) \psi + \frac{f_\pi^2}{4} \text{Tr} \left[(\partial^\mu U)^\dagger (\partial_\mu U) + \chi U^\dagger + U \chi^\dagger \right]. \quad (170)$$

Here, ψ is the nucleon Dirac field, and the matrix-valued field

$$U \equiv \exp \left(i \frac{\vec{\tau} \cdot \vec{\pi}}{f_\pi} \right) \quad (171)$$

collects the pion fields in an exponential representation. D_μ here is the so-called chiral covariant derivative that couples the pion field to the nucleons. The matrix

$$\chi = 2B_0 \text{diag}(m_q, m_q), \quad (172)$$

where m_q is the light quark mass (in the exact isospin limit, $m_u = m_d = m_q$) contains the effect from explicit chiral symmetry breaking. Via the Gell-Mann–Oakes–Renner relation,

$$m_\pi^2 = 2B_0 m_q, \quad (173)$$

one can show that χ generates a mass term for the pion field.

10. Exercise: Expand the exponential in Eq. (171) to show that $\frac{f_\pi^2}{4} \text{Tr}[(\partial^\mu U)^\dagger (\partial_\mu U)]$ generates a kinetic term for the pion field $\vec{\pi}$ plus higher-order pion self interactions.

After a couple of steps, which we encourage the reader to follow based on the definitions given in Ref. [44], the leading terms in the Lagrangian are found to be

$$\begin{aligned} \mathcal{L}_{\pi N}^{(1)} + \mathcal{L}_2^\pi = & \bar{\psi} (i\not{\partial} - M_N) \psi + \frac{1}{2} (\partial^\mu \vec{\pi}) \cdot (\partial_\mu \vec{\pi}) - \frac{1}{2} m_\pi^2 \vec{\pi}^2 \\ & - \frac{g_A}{2f_\pi} \bar{\psi} \gamma^\mu \gamma^5 (\vec{\tau} \cdot \partial_\mu \vec{\pi}) \psi + \frac{i}{8f_\pi^2} \bar{\psi} \gamma^\mu (\vec{\tau} \cdot \vec{\pi}) (\vec{\tau} \cdot \partial_\mu \vec{\pi}) \psi + \dots \end{aligned} \quad (174)$$

Comparing this to our pseudoscalar model (28) in Sec. 2.2.2, we see that the pion-nucleon coupling now comes with explicit derivatives, as required by chiral symmetry. After a Foldy-Wouthuysen transformation, however, one-pion-exchange in the nonrelativistic limit gives the same structure as in Eq. (49). There is no explicit σ field in Eq. (174); in the chiral theory, this particle only appears as a resonance generated by two-pion exchange.

Acknowledgements We thank Dick Furnstahl and Bira van Kolck and for various stimulating discussions. Moreover, SK is grateful to Martin Hoferichter for the insights into Coulomb-gauge quantization presented in Sec. 5.1.

References

1. K.G. Wilson, Rev. Mod. Phys. **55**, 583 (1983)
2. G.P. Lepage, What is renormalization? (1989). hep-ph/0506330
3. S. Weinberg, Physica A **96**, 327 (1979)
4. D.B. Kaplan, Effective field theories (1995). nucl-th/9506035
5. D.B. Kaplan, Five lectures on effective field theory (2005). nucl-th/0510023
6. J. Gasser, H. Leutwyler, Ann. Phys. **158**, 142 (1984)
7. J. Gasser, H. Leutwyler, Nucl. Phys. B **250**, 465 (1985)
8. J.F. Donoghue, E. Golowich, B.R. Holstein, *Dynamics of the standard model* (Cambridge University Press, 1992)
9. E. Jenkins, A.V. Manohar, Phys. Lett. B **255**, 558 (1991)
10. A. Gardestig, K. Kubodera, F. Myhrer, Phys. Rev. C **76**, 014005 (2007)
11. P.R. Hagen, Effective field theory for halo nuclei. Ph.D. thesis, Bonn University (2014)
12. E. Braaten, H.W. Hammer, Phys. Rep. **428**, 259 (2006)
13. S.R. Beane, P.F. Bedaque, W.C. Haxton, D.R. Phillips, M.J. Savage, *At The Frontier of Particle Physics* (World Scientific, 2001), *Handbook of QCD*, vol. 1, chap. From hadrons to nuclei: Crossing the border, p. 133
14. C.A. Bertulani, H.W. Hammer, U. van Kolck, Nucl. Phys. A **712**, 37 (2002)
15. P.F. Bedaque, H.W. Hammer, U. van Kolck, Phys. Lett. B **569**, 159 (2003)
16. U. van Kolck, Nucl. Phys. A **645**, 273 (1999)
17. D.B. Kaplan, M.J. Savage, M.B. Wise, Nucl. Phys. B **534**, 329 (1998)
18. D.B. Kaplan, Nucl. Phys. B **494**, 471 (1997)
19. G.V. Skornikov, K.A. Ter-Martirosian, Sov. Phys. JETP **4**, 648 (1957)
20. G. Danilov, Sov. Phys. JETP **13**, 349 (1961)

21. V.F. Kharchenko, Sov. J. Nucl. Phys. **16**, 173 (1973)
22. P.F. Bedaque, H.W. Hammer, U. van Kolck, Phys. Rev. Lett. **82**, 463 (1999)
23. V. Efimov, Phys. Lett. B **33**, 563 (1970)
24. E. Braaten, D. Kang, L. Platter, Phys. Rev. Lett. **106**, 153005 (2011)
25. F. Ferlaino, R. Grimm, Physics **3**, 9 (2010)
26. J. Ulmanis, S. Häfner, R. Pires, F. Werner, D.S. Petrov, E.D. Kuhnle, M. Weidemüller, Phys. Rev. A **93**, 022707 (2016)
27. P.F. Bedaque, H.W. Hammer, U. van Kolck, Nucl. Phys. A **646**, 444 (1999)
28. S. König, H.W. Griesshammer, H.W. Hammer, J. Phys. G **42**, 045101 (2015)
29. P.F. Bedaque, H.W. Hammer, U. van Kolck, Nucl. Phys. A **676**, 357 (2000)
30. M.E. Peskin, D.V. Schroeder, *An Introduction to Quantum Field Theory* (Westview Press, 1995)
31. S. Weinberg, Phys. Lett. B **251**, 288 (1990)
32. S. Weinberg, Nucl. Phys. B **363**, 3 (1991)
33. D.B. Kaplan, M.J. Savage, M.B. Wise, Nucl. Phys. B **478**, 629 (1996)
34. D.B. Kaplan, M.J. Savage, M.B. Wise, Phys. Lett. B **424**, 390 (1998)
35. S. Fleming, T. Mehen, I.W. Stewart, Nucl. Phys. A **677**, 313 (2000)
36. P.F. Bedaque, U. van Kolck, Ann. Rev. Nucl. Part. Sci. **52**, 339 (2002)
37. A. Nogga, R.G.E. Timmermans, U. van Kolck, Phys. Rev. C **72**, 054006 (2005)
38. M.C. Birse, Phys. Rev. C **74**, 014003 (2006)
39. E. Epelbaum, H.W. Hammer, U.G. Meißner, Rev. Mod. Phys. **81**, 1773 (2009)
40. R. Machleidt, D.R. Entem, Phys. Rep. **503**, 1 (2011)
41. E. Epelbaum, U.G. Meißner, Few Body Syst. **54**, 2175 (2013)
42. H.W. Hammer, A. Nogga, A. Schwenk, Rev. Mod. Phys. **85**, 197 (2013)
43. B. Long, Y. Mei, Phys. Rev. C **93**, 044003 (2016)
44. S. Scherer, M.R. Schindler, Lect. Notes Phys. **830**, 1 (2012)